

Supplementary Information for

**A pyridine oxide-decorated covalent organic framework for catalysis allylation of aromatic aldehydes with allyl(trichloro)silane**

Jian-Cheng Wang<sup>†\*</sup>, Ru Pan<sup>†</sup>, Wen-Ting Yang<sup>†</sup>, Zhi Chen, Jia-Qi Du, Jing-Lan Kan and Yu-Bin Dong\*

College of Chemistry, Chemical Engineering and Materials Science, Collaborative Innovation Centre of Functionalized Probes for Chemical Imaging in Universities of Shandong, Key Laboratory of Molecular and Nano Probes, Ministry of Education, Shandong Normal University, Jinan 250014, P. R. China.

E-mail: wangjiancheng1003@163.com, yubindong@sdu.edu.cn (Y.B. Dong).

<sup>†</sup>These authors contributed equally.

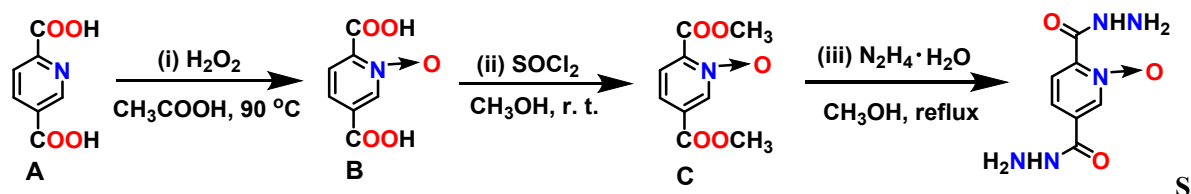
**Contents**

1. General information (page S2)
2. Synthesis and characterization of 2,5-di(hydrazinecarbonyl)pyridine-1-oxide (page S2)
3. Synthesis and characterization of Py-O-COF (page S4)
4. GC analysis and product characterization for optimization of reaction conditions for the model allylation of aromatic aldehyde (Table 1) (page S8)
5. Synthesis and characterization of Py-COF (page S12)
6. The solid-state <sup>15</sup>N NMR spectra of Py-O-COF and Py-COF (page S17)
7. A possible reaction mechanism of Py-O-COF-catalyzed the allylation of benzaldehyde (page S18)
8. GC analysis for five catalytic runs of the allylation of benzaldehyde and N<sub>2</sub> adsorption isotherms for Py-O-COF at 77 K before and after five catalytic runs (page S18)
9. Comparison of Py-O-COF with some reported catalysts for allylation of aromatic aldehyde (page S19)
10. GC analysis for the reactions Py-O-COF-catalyzed different substituted aromatic aldehydes and allyl trichlorosilane as substrates (Table 2) (page S19)
11. Products characterization for the Py-O-COF catalyzed allylation of aromatic aldehyde (page S22)
12. Reference (page S25)

## 1. General information

All the chemicals were obtained from commercial sources and used without further purification. **2,5-di(hydrazinecarbonyl)pyridine-1-oxide** (Scheme S1) and **pyridine-2,5-dicarbohydrazide** (Scheme S2) were synthesized according to literature method.<sup>1, 2</sup> Infrared (IR) spectra were obtained in the 400–4000  $\text{cm}^{-1}$  range using a Bruker ALPHA FT-IR Spectrometer.  $^1\text{H}$  NMR data were collected on an AM-400 spectrometer. Chemical shifts are reported in  $\delta$  relative to TMS. MS spectra were obtained by Bruker maxis ultra-high resolution-TOF MS system. GC-MS analysis data were performed on a gas chromatographic (Agilent GC8890/5977B GC/MSD). The GC capillary columns (DB-WAX, 30 m length  $\times$  0.53 mm; HP-5, 30 m length  $\times$  0.32 mm) were purchased from the Agilent Technologies. Thermogravimetric analyses (TGA) were carried out on a TA Instrument Q5 simultaneous TGA under flowing nitrogen at a heating rate of  $5^\circ\text{C}/\text{min}$ . PXRD patterns were obtained on D8 Advance X-ray powder diffractometer with Cu  $K\alpha$  radiation ( $\lambda = 1.5405 \text{ \AA}$ ). HR-TEM (High Resolution Transmission Electron Microscopy) analyses were performed on a JEOL 2100 Electron Microscope at an operating voltage of 200 kV. The total surface areas of the COFs were measured by the BET (Brunauer Emmer Teller) isotherms using  $\text{N}_2$  adsorption at 77 K and this was done on the Micromeritics ASAP 2020 sorption/desorption analyzer.  $^{13}\text{C}$  CP-MAS solid-state NMR spectra were recorded on a MERCURY plus 400 spectrometers operating at resonance frequencies of 400 MHz. The scanning electron microscopy (SEM) micrographs were recorded on a Gemini Zeiss Supra TM scanning electron microscope equipped with energy-dispersive X-ray detector (EDX). XPS spectra were obtained from THI5300 (PE).

## 2. Synthesis and characterization of 2,5-di(hydrazinecarbonyl)pyridine-1-oxide



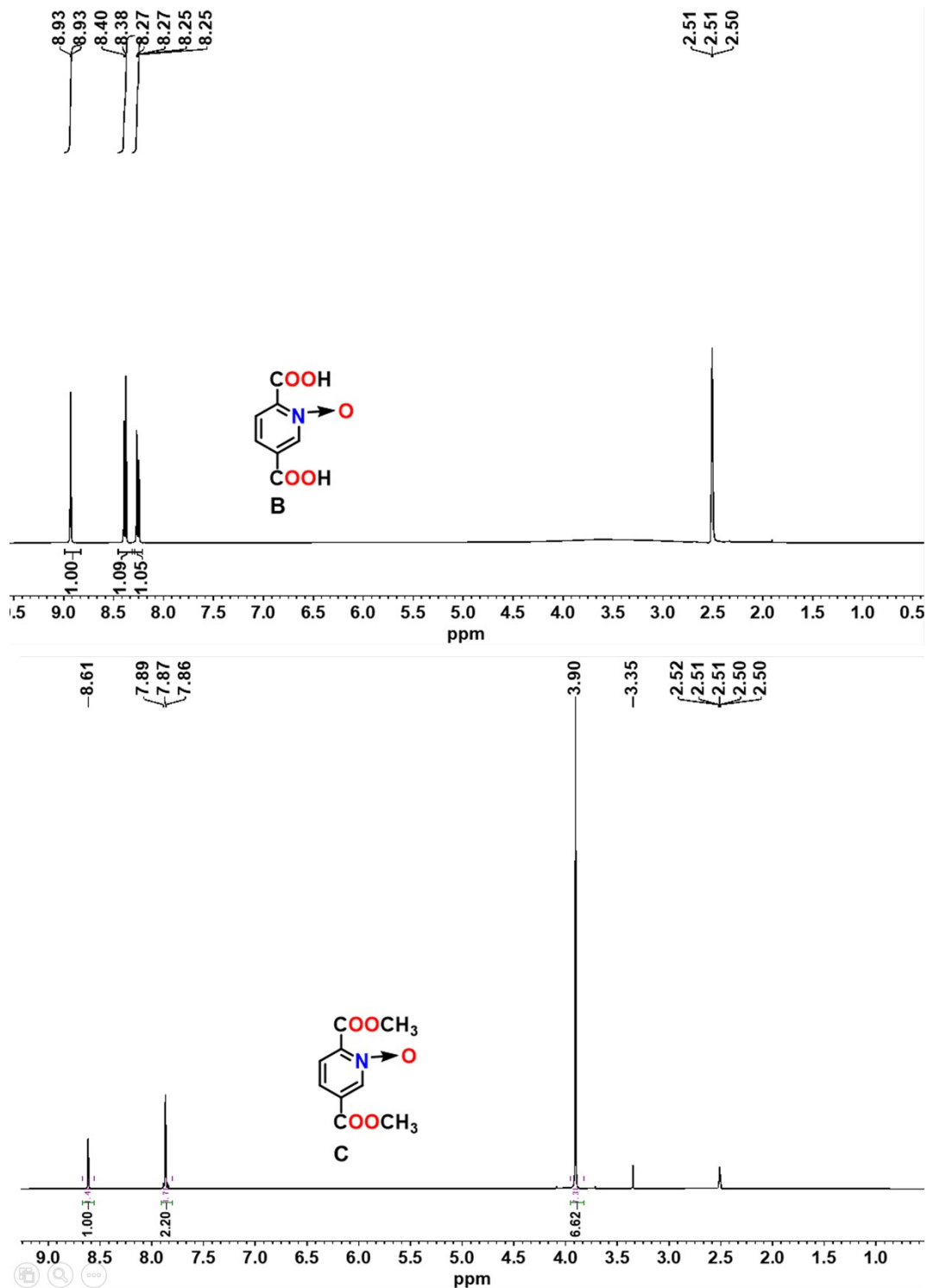
**Scheme S1** Synthesis of **2,5-di(hydrazinecarbonyl)pyridine-1-oxide**

(i) A mixture of **A** (1.67 g, 10.0 mmol) and 30%  $\text{H}_2\text{O}_2$  (10 mL) was refluxed at  $90^\circ\text{C}$  for 10 h in  $\text{CH}_3\text{COOH}$  (10 mL). Upon completion of the reaction, filter the reaction mixture to obtain a filter cake, and subsequently wash the collected filter cake with water several times to yield product **B** as white solid in 64% yield (1.17 g). IR (KBr pellet  $\text{cm}^{-1}$ ): 3082 (s), 1722 (vs), 1640 (s), 1614 (s), 1562 (w), 1504 (s), 1412 (s), 1298 (w), 1227 (s), 1092 (w), 945 (w), 920 (w), 887 (s), 755 (s).  $^1\text{H}$  NMR (400 MHz,  $\text{DMSO}-d_6$ )  $\delta$  8.93 (s, 1H), 8.39 (d,  $J = 8.0$  Hz, 1H), 8.26 (dd,  $J = 8.0$  Hz, 1H).  $^{13}\text{C}$  NMR (101 MHz,  $\text{DMSO}-d_6$ )  $\delta$  163.62, 160.96, 140.01, 139.00, 133.35, 132.60, 129.24. HRMS (ESI)  $m/z$   $[\text{M}+\text{H}]^+$  calcd for  $\text{C}_7\text{H}_6\text{NO}_5^+$  184.0246, found 184.0224.

(ii) In  $\text{N}_2$ , a mixture of **B** (0.92 g, 5 mmol) and  $\text{SOCl}_2$  (5 mL) was stirred at  $25^\circ\text{C}$  for 12 h in methanol (20 mL). The product was extracted by ethyl acetate and purified by column on silica gel (petroleum ether/ethyl acetate = 3:1) to afford **C** as the yellow solid in 73% yield (0.77 g). IR (KBr pellet  $\text{cm}^{-1}$ ): 1744 (s), 1731 (vs), 1656 (w), 1633 (w), 1435 (s), 1387 (s), 1320 (s), 1239 (s), 1214 (s), 1119 (s), 986 (w), 752 (s).  $^1\text{H}$  NMR (400 MHz,  $\text{DMSO}-d_6$ )  $\delta$  8.61 (s, 1H), 7.87 (m, 2H), 3.90 (s, 6H).  $^{13}\text{C}$  NMR (101 MHz,  $\text{DMSO}-d_6$ )  $\delta$  162.64, 144.71, 140.47, 130.80, 126.02, 53.67. HRMS (ESI)  $m/z$   $[\text{M}+\text{H}]^+$  calcd for  $\text{C}_9\text{H}_{10}\text{NO}_5^+$  212.0559, found 212.0561.

(iii) A mixture of **C** (0.22 g, 1.0 mmol) and hydrazine hydrate (0.62 mL, 10.0 mmol) was stirred at  $65^\circ\text{C}$  for 24 h in methanol (20 mL). Upon completion of the reaction, the solvent is evaporated under reduced

pressure to yield the crude product, which is subsequently washed several times with methanol to obtain product **2,5-di(hydrazinecarbonyl)pyridine-1-oxide** as white solid in 80% yield (0.18 g). IR (KBr pellet  $\text{cm}^{-1}$ ): 3203 (s), 3174 (s), 3045(w), 1760 (vs), 1651 (s), 1621 (s), 1514 (s), 1477 (s), 1383 (s), 1195 (s), 987 (s), 831 (s), 714 (s), 651 (s).  $^1\text{H}$  NMR (400 MHz,  $\text{DMSO-}d_6$ )  $\delta$  11.95 (s, 1H), 10.19 (s, 1H), 8.72 (d,  $J = 4.0$  Hz, 1H), 8.26 (d,  $J = 12.0$  Hz, 1H), 7.93 (dd,  $J = 8.0$  Hz, 1H), 4.85 (m, 4H).  $^{13}\text{C}$  NMR (101 MHz,  $\text{DMSO-}d_6$ )  $\delta$  157.05, 141.39, 140.50, 139.57, 127.99, 126.18. HRMS (ESI)  $m/z$   $[\text{M}+\text{H}]^+$  calcd for  $\text{C}_7\text{H}_{10}\text{N}_5\text{O}_3^+$  212.0784, found 212.0765.



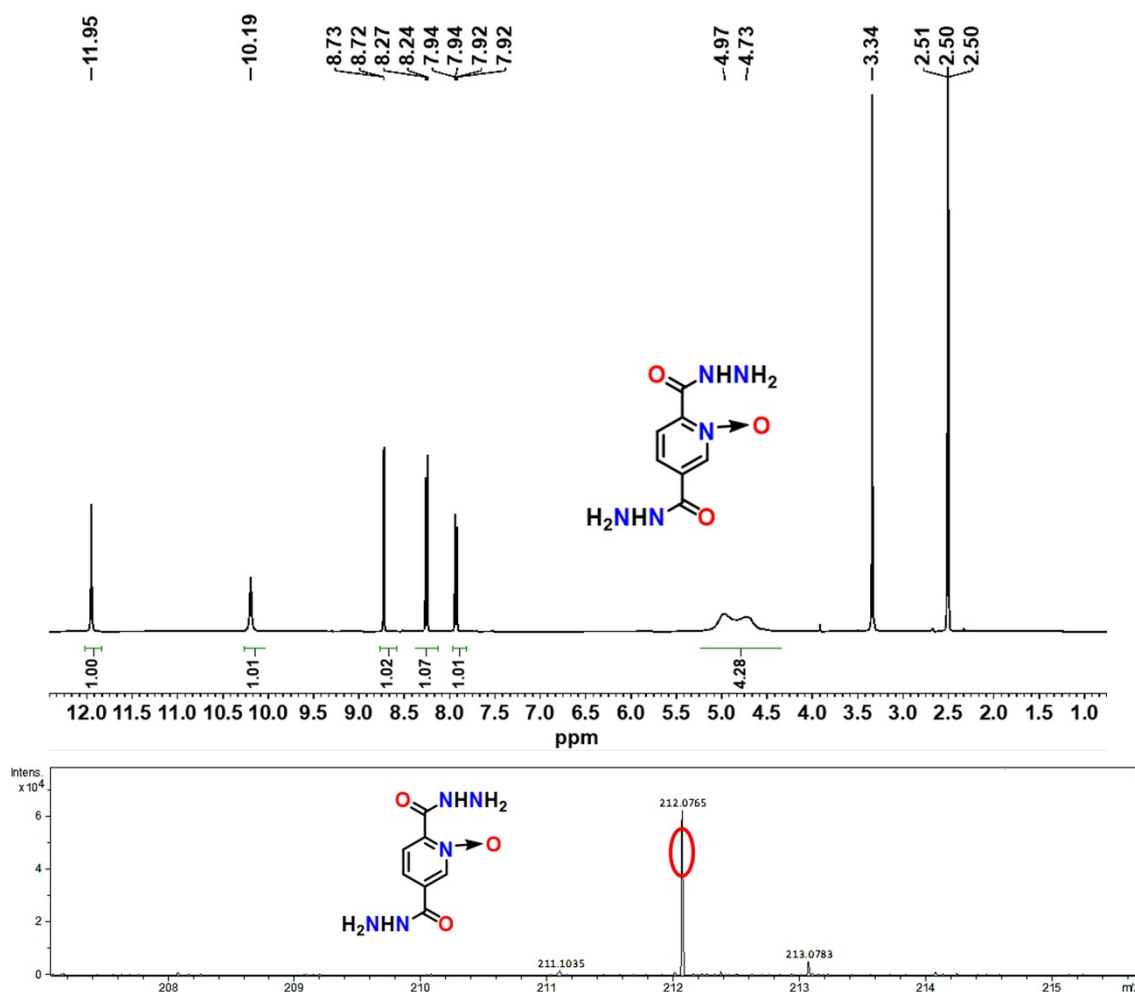


**Fig. S1.** <sup>1</sup>H NMR spectra of **B**, **C** and **2,5-di(hydrazinecarbonyl)pyridine-1-oxide** and HR-MS of **2,5-di(hydrazinecarbonyl)pyridine-1-oxide**

### 3. Synthesis and characterization of Py-O-COF

A mixture of **2,5-di(hydrazinecarbonyl)pyridine-1-oxide** (31.6 mg, 0.15 mmol), acetic acid (0.3 mL, 6.0 M), 2,4,6-trihydroxy-1,3,5-benzenetricarbaldehyde (21.0 mg, 0.10 mmol) and N, N-dimethyl acetamide/methanol (1.5/0.5 mL) was capped in a Pyrex tube with a flame and heated at 120 °C for 3 days. The obtained precipitate was collected by centrifugation and washed with methanol, N, N-dimethyl formamide and ethanol, respectively. The collected solid was then dried in vacuo overnight to yield **Py-O-COF** (20.5 mg, 64% yield). IR (KBr pellet cm<sup>-1</sup>): 3366 (s), 2973 (s), 1658 (s), 1629 (s), 1590 (vs), 1483 (w), 1385 (s), 1331 (s), 1189 (w), 1088 (w), 1047 (s), 879 (w), 662 (w).

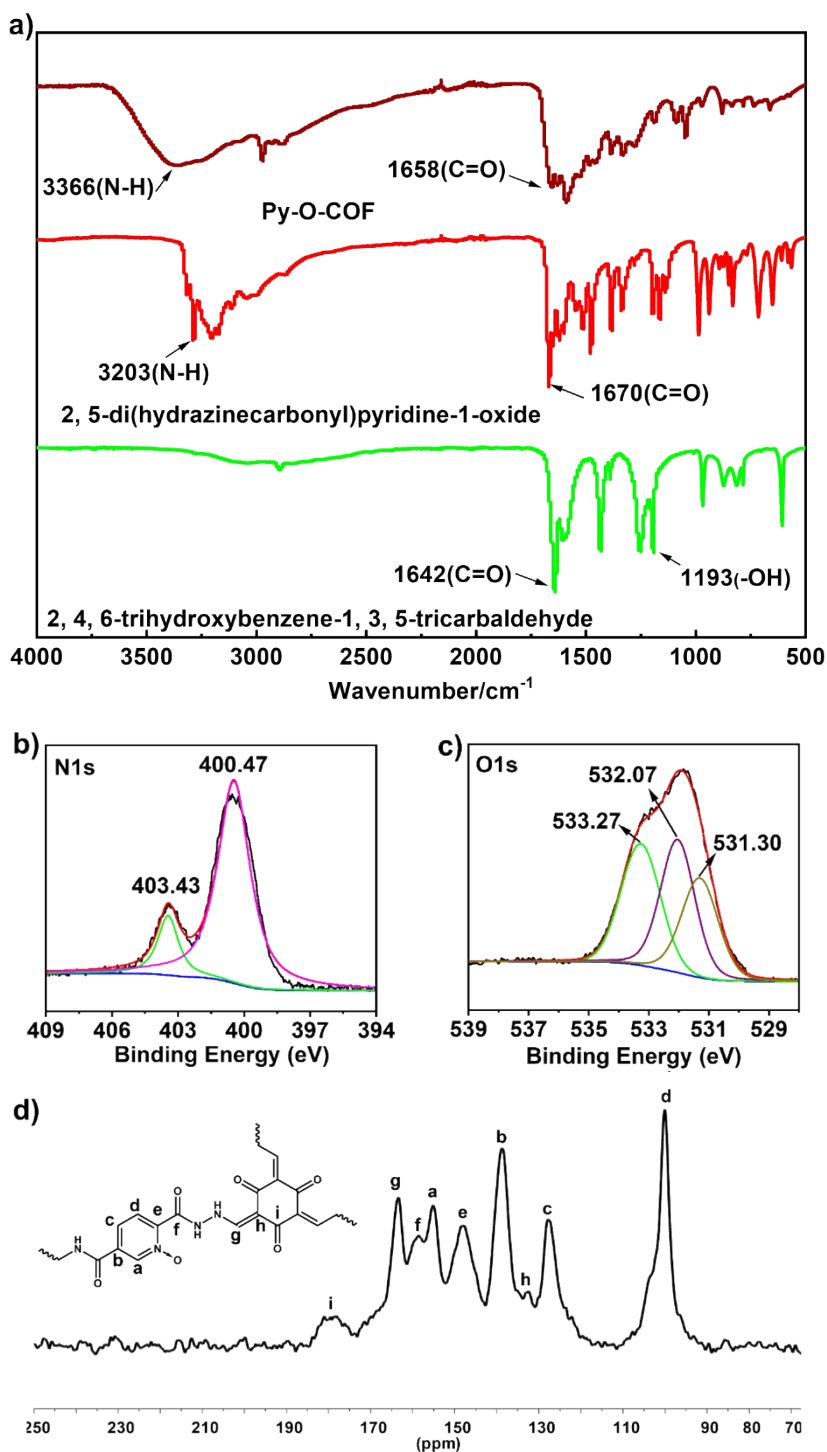


**Fig. S2.** a) The FT-IR spectra of **Py-O-COF** and its monomers. The Fourier transform infrared (FT-IR) spectra showed all characteristic peaks, such as 1658 cm<sup>-1</sup> for [-C=O], 3366 cm<sup>-1</sup> for [-N-H] stretching vibrations, which suggested the formation of **Py-O-COF** through the Schiff base condensation reaction. b) The XPS spectrum of N species in **Py-O-COF**. The XPS spectrum of N species in **Py-O-COF** showed that deconvolution of the N 1s spectrum resulted in two peaks at 403.43 and 400.47 eV, which can be attributed to the nitrogen atoms bound to carbon (i.e., N-C) and to oxygen (i.e., N-O), respectively.<sup>3</sup> c) The XPS spectrum of O species in **Py-O-COF**. The XPS spectrum of O species in **Py-O-COF** showed that deconvolution of the O 1s spectrum also resulted in three peaks at 533.27, 532.07 and 531.30 eV, which can be attributed to the oxygen atoms bound to carbon (i.e., O=C) and to nitrogen (i.e., N-O),

respectively.<sup>4</sup> d) The solid-state <sup>13</sup>C-MAS NMR spectrum of **Py-O-COF**,  $\delta$  (ppm): 178.1, 163.3, 158.6, 155.1, 147.7, 138.7, 132.4, 127.8, 100.0. The formation of **Py-O-COF** was verified by the existence of the keto, hydrazide, acylhydrazinyl, pyridine oxide and alkene in **Py-O-COF** through the corresponding resonances at 178.1, 163.3, 158.6, 155.6-122.8, 100.0 ppm, respectively.

**Table S1.** Fractional atomic coordinates for the unit cell of **Py-O-COF**

**Py-O-COF** AA stacking mode, space group: *P3*

$a = b = 30.1561 \text{ \AA}$ ,  $c = 3.5270 \text{ \AA}$

$\alpha = \beta = 90^\circ$ ,  $\gamma = 120^\circ$

Aotm	x	y	z
C1	-0.69968	-0.39003	0.16214
C2	-0.6432	-0.36588	0.12178
C3	-0.73064	-0.44066	0.22624
O4	-0.62403	-0.39188	0.03826
N5	-0.71223	-0.47474	0.32468
N6	-0.74525	-0.528	0.3008
C7	-0.73115	-0.56202	0.43069
C8	-0.76684	-0.6181	0.41104
C9	-0.74711	-0.65036	0.3264
C10	-0.77979	-0.70312	0.30759
C11	-0.83226	-0.724	0.37427
C12	-0.85069	-0.69067	0.45827
N13	-0.81824	-0.63917	0.48061
O14	-0.68815	-0.5463	0.55689
O15	-0.83781	-0.60945	0.59208
C16	-0.868	-0.77987	0.35435
N17	-0.85347	-0.81387	0.48005
N18	-0.8854	-0.86744	0.46802
C19	-0.93827	-0.89263	0.58366
C20	-0.96658	-0.9434	0.65595
O21	-0.91056	-0.79528	0.22155
C22	-0.94417	-0.9772	0.70159
O23	0.10043	0.04077	0.79765
H24	0.32356	0.53959	0.45269
H25	0.2194	0.45836	0.16683

H26	0.29331	0.36528	0.26966
H27	0.23591	0.27271	0.23237
H28	0.10894	0.29393	0.51656
H29	0.87014	0.9131	0.59748
H30	0.79993	0.98398	0.57366
H31	0.97947	0.86819	0.39258
H32	0.45653	0.68476	0.22381

**Table S2.** Fractional atomic coordinates for the unit cell of **Py-O-COF**

**Py-O-COF** AB stacking mode, space group:  $P6_3$

$a = b = 30.2316 \text{ \AA}$ ,  $c = 6.8186 \text{ \AA}$

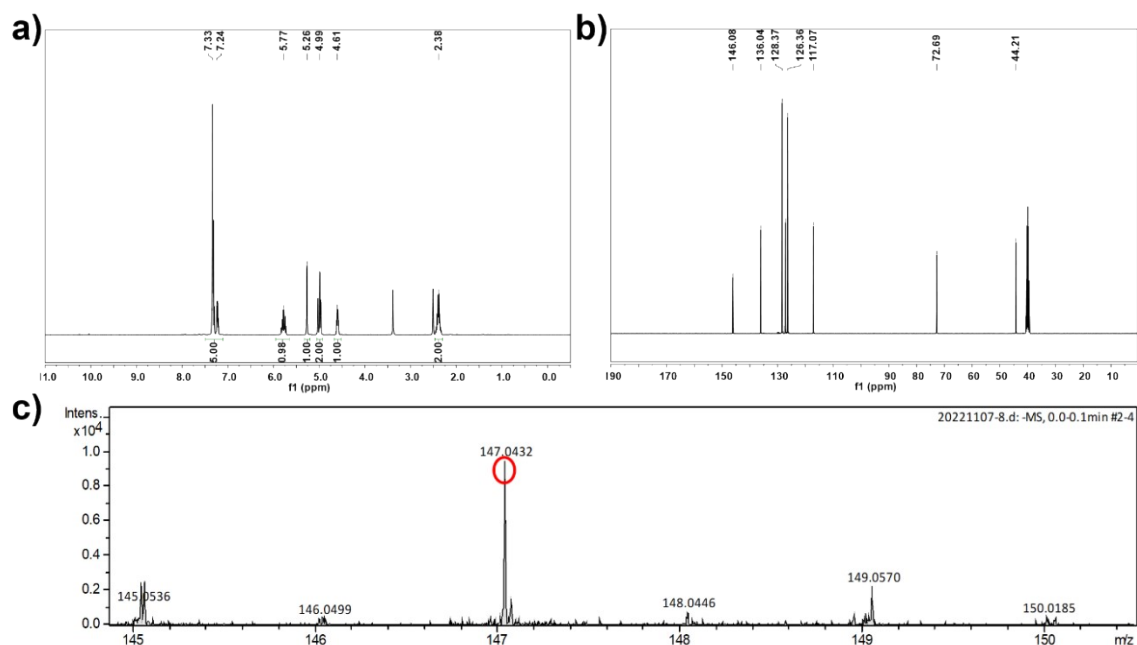
$\alpha = \beta = 90^\circ$ ,  $\gamma = 120^\circ$

Aotm	x	y	z
C1	-0.69969	-0.38991	0.31593
C2	-0.64332	-0.3659	0.29547
C3	-0.73056	-0.44048	0.34792
O4	-0.62429	-0.39198	0.25306
N5	-0.71207	-0.47427	0.40042
N6	-0.74394	-0.52736	0.37866
C7	-0.73131	-0.56147	0.45588
C8	-0.76561	-0.61731	0.43208
C9	-0.74408	-0.64818	0.39424
C10	-0.77562	-0.70062	0.36913
C11	-0.82872	-0.72255	0.38224
C12	-0.84892	-0.6906	0.42149
N13	-0.81763	-0.63943	0.44813
O14	-0.6908	-0.54599	0.54187
O15	-0.83917	-0.61117	0.50011
C16	-0.86327	-0.77801	0.35323
N17	-0.8502	-0.81282	0.42023
N18	-0.88157	-0.86587	0.39539
C19	-0.93501	-0.89187	0.4455
C20	-0.96499	-0.94335	0.45975
O21	-0.90355	-0.79244	0.26698

C22	-0.94418	-0.97871	0.47184
O23	0.10132	0.0383	0.50017
H24	0.3228	0.54007	0.4736
H25	0.22274	0.45922	0.29552
H26	0.29691	0.36836	0.38113
H27	0.24158	0.27634	0.33506
H28	0.11011	0.29315	0.43523
H29	0.86855	0.91599	0.46374
H30	0.79991	0.98565	0.48258
H31	0.97879	0.86426	0.33876
H32	0.45649	0.68487	0.34487

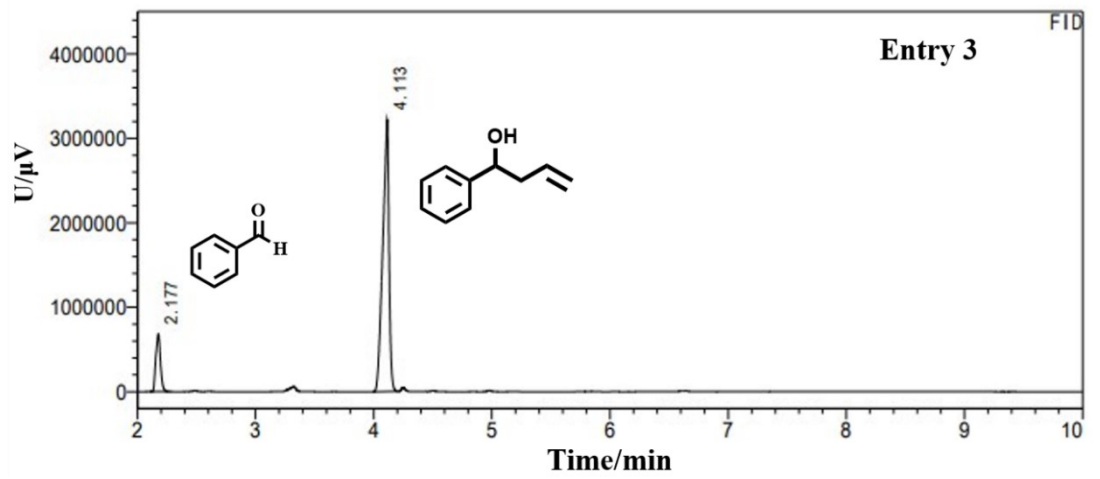
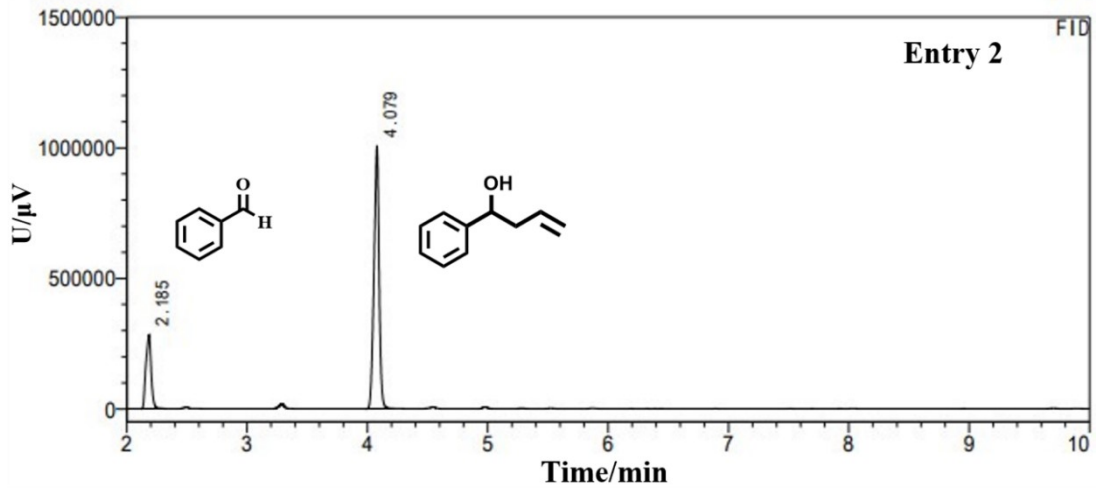
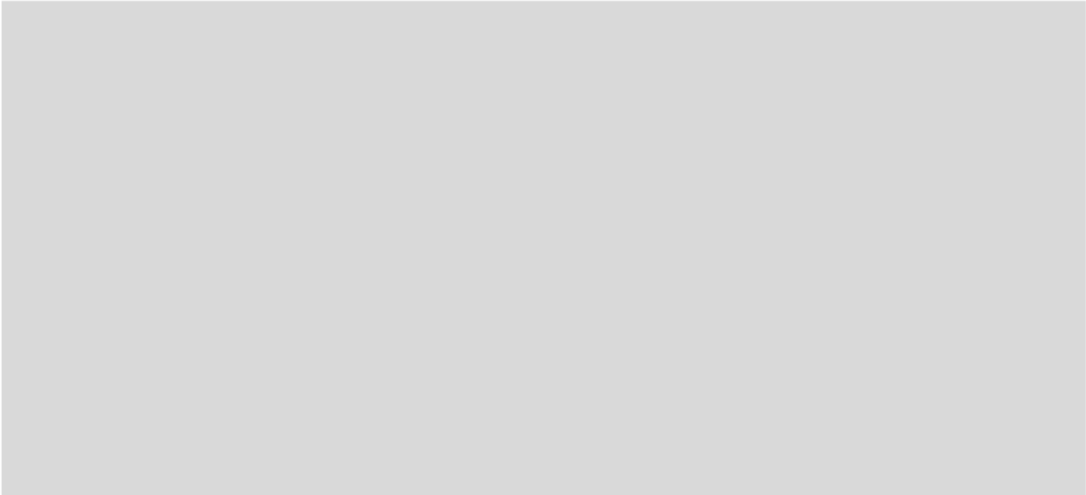
#### 4. GC analysis and product characterization for optimization of reaction conditions for the model allylation of aromatic aldehyde (Table 1)

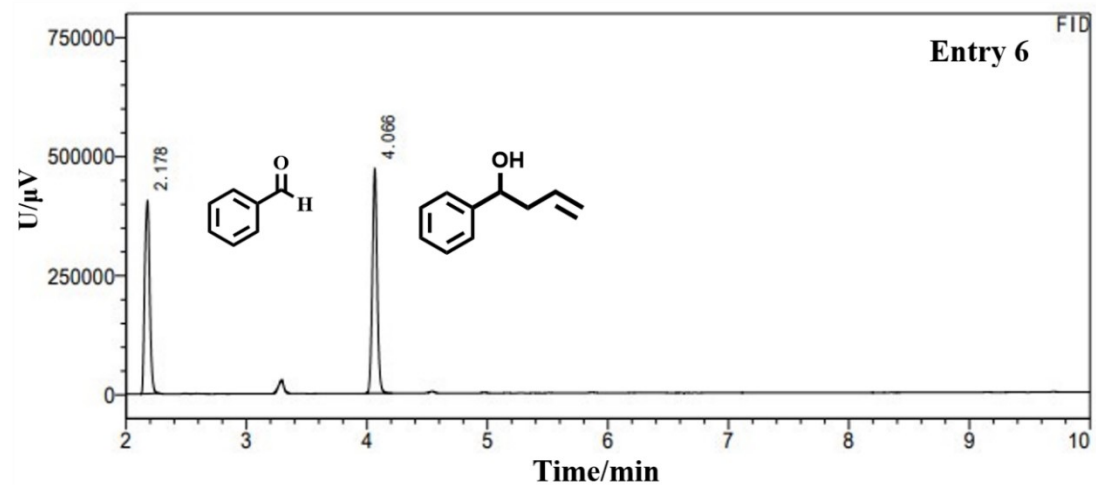
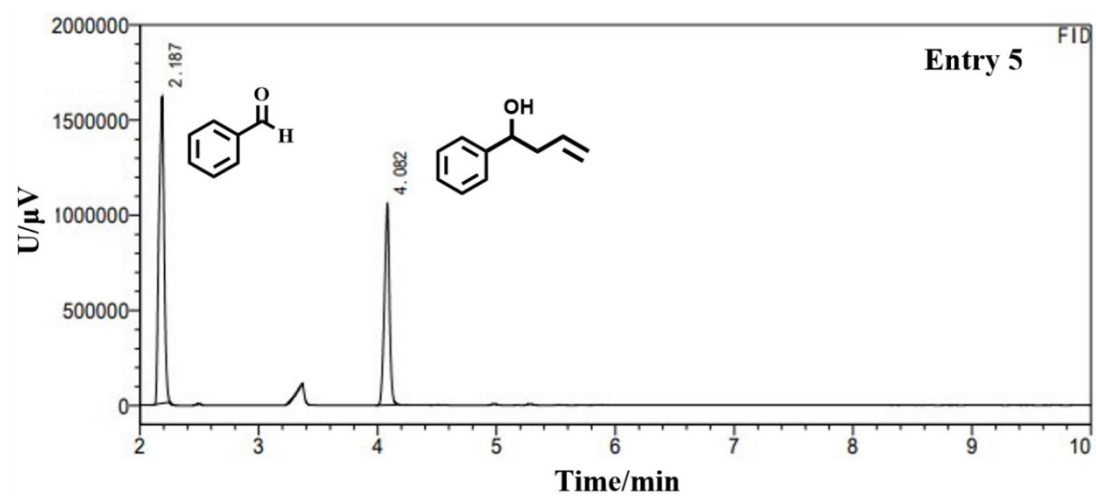
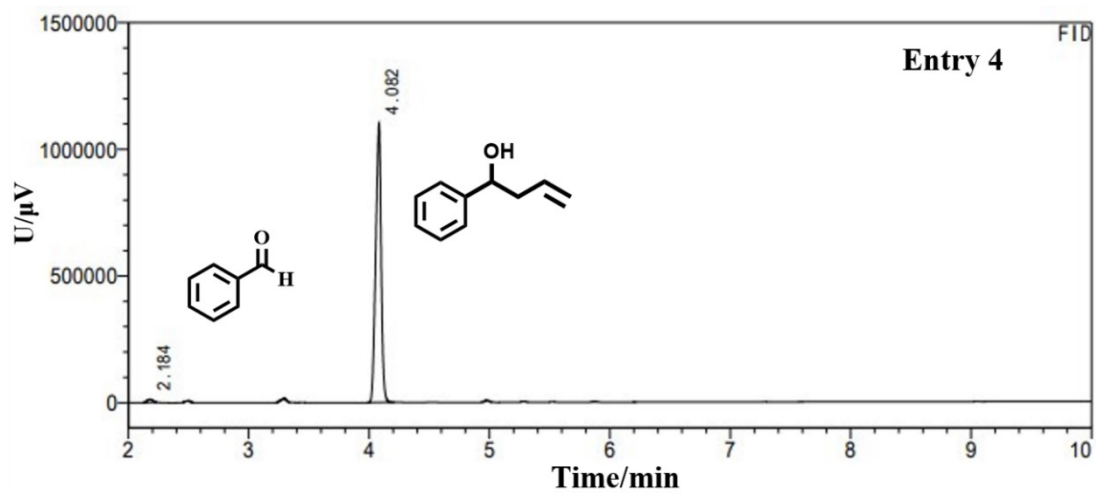
In nitrogen, a mixture of phenylaldehyde (0.30 mmol), allyltrichlorosilane (0.36 mmol), DIPEA (0.90 mmol, N, N-diisopropylethylamine), catalyst (5-25 mg), and CH<sub>3</sub>CN (2.0 mL) was stirred at 25 °C for 48 h. GC was used to monitor the reaction progress. The mixture was quenched with saturated brine and extracted with ethyl acetate. Then, the combined organic layers were evaporated in vacuo and the resulting residue was purified by silica gel chromatography (petroleum ether /ethyl acetate = 3/1).

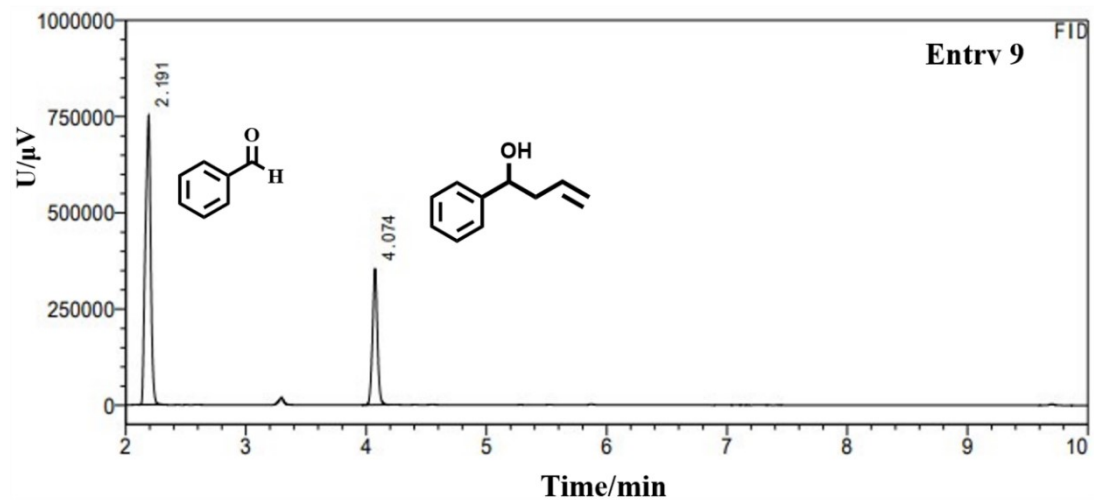
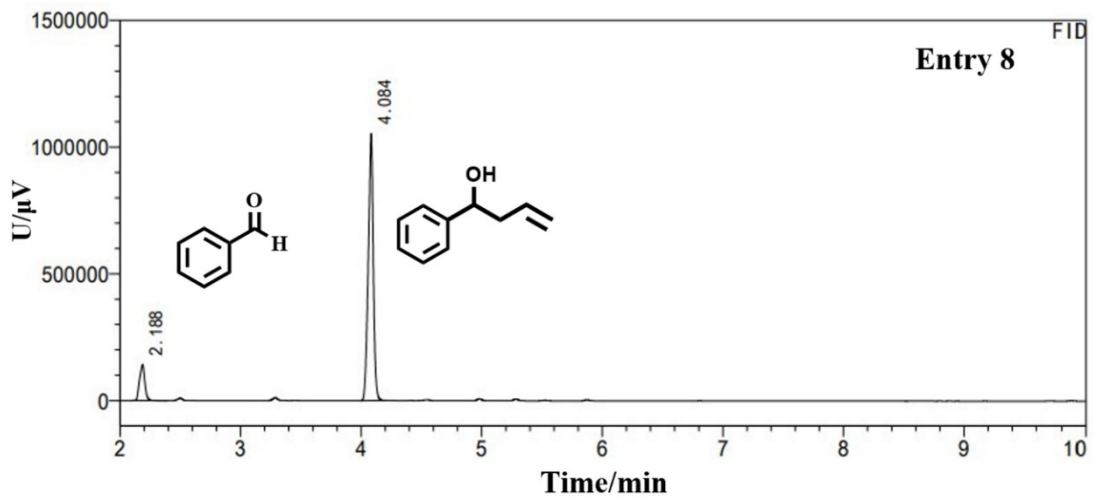
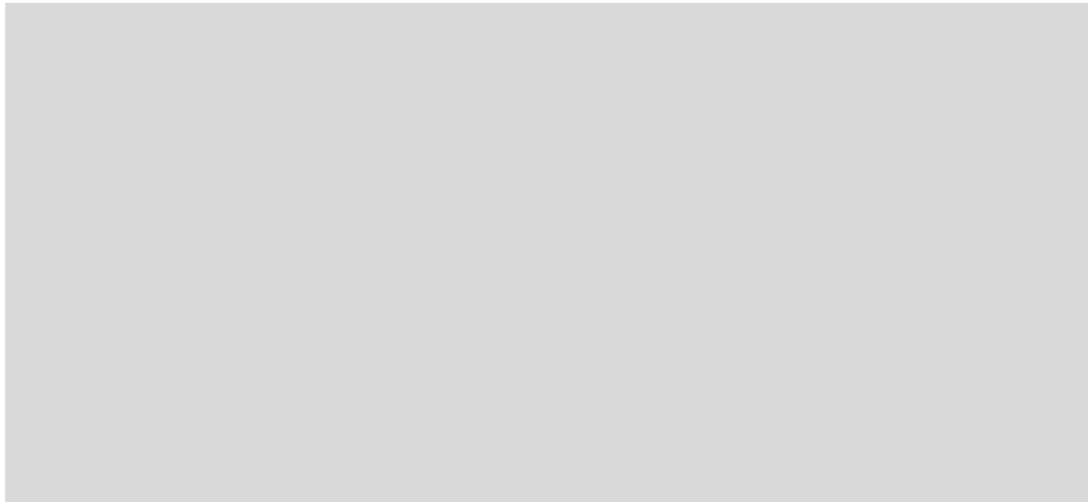




d)







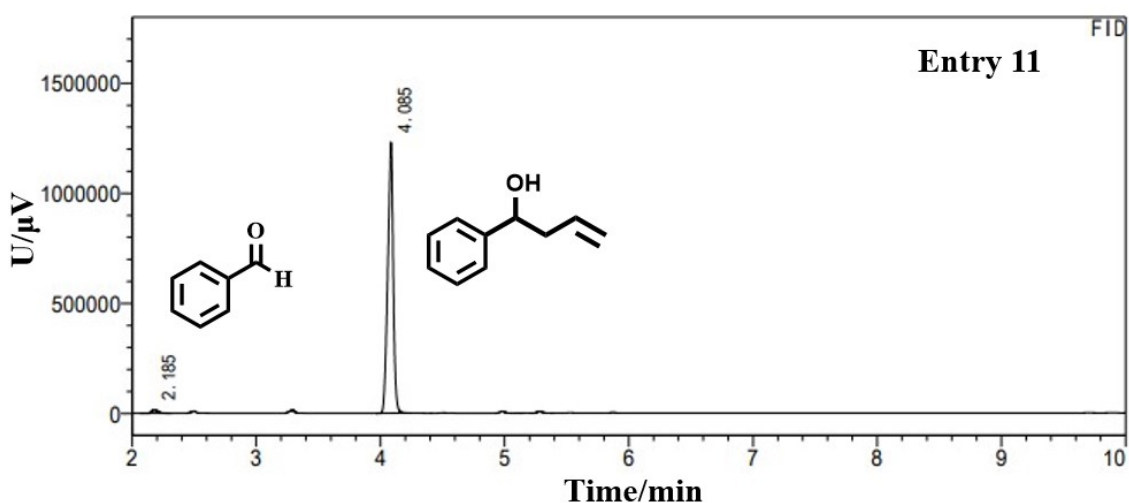
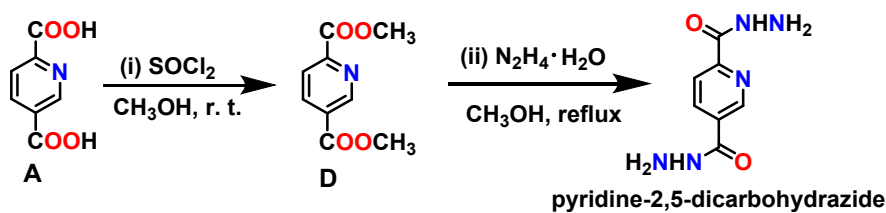


**Fig. S3.** (a)  $^1\text{H}$  NMR spectrum of the model allylation reaction product.  $^1\text{H}$  NMR (400 MHz,  $\text{DMSO-}d_6$ )  $\delta$  7.28 (d,  $J = 36.1$  Hz, 5H), 5.77 (s, 1H), 5.26 (s, 1H), 4.99 (s, 2H), 4.61 (s, 1H), 2.38 (s, 2H). (b)  $^{13}\text{C}$  NMR spectrum of the model allylation reaction product.  $^{13}\text{C}$  NMR (101 MHz,  $\text{DMSO-}d_6$ )  $\delta$  146.08, 136.04, 128.37, 127.15, 126.36, 117.07, 72.69, 44.21. (c) MS spectrum of the model allylation reaction product. HRMS (ESI):  $m/z$  [M-H] $^-$ , Calcd for  $\text{C}_{10}\text{H}_{11}\text{O}$  147.0815, found 147.0432. (d) The GC analysis of the yields of the model allylation reaction.

## 5. Synthesis and characterization of Py-COF

### (1) Synthesis and characterization of pyridine-2,5-dicarbohydrazide



**Scheme S2** Synthesis of pyridine-2,5-dicarbohydrazide

(i) In  $\text{N}_2$ , a mixture of **A** (0.80 g, 5.0 mmol) and  $\text{SOCl}_2$  (5 mL) was stirred at room temperature for 12 h in methanol (20 mL). The product was extracted by ethyl acetate and purified by column on silica gel

(petroleum ether/ethyl acetate, 3:1). **D** was obtained as the white solid in 71% yield (0.70 g). IR (KBr pellet  $\text{cm}^{-1}$ ): 1713 (vs), 1435 (s), 1383 (s), 1285 (s), 1249 (s), 1197 (w), 1128 (s), 1018 (s), 953 (s), 741 (s).  $^1\text{H}$  NMR (400 MHz,  $\text{DMSO-}d_6$ )  $\delta$  9.18 (dd,  $J = 2.1, 0.7$  Hz, 1H), 8.48 (dd,  $J = 8.1, 2.2$  Hz, 1H), 8.19 (dd,  $J = 8.1, 0.7$  Hz, 1H), 3.92 (d,  $J = 2.7$  Hz, 6H).  $^{13}\text{C}$  NMR (101 MHz,  $\text{DMSO-}d_6$ )  $\delta$  165.00, 150.44, 138.93, 128.68, 125.30, 53.25. HRMS (ESI)  $m/z$   $[\text{M}+\text{H}]^+$  calcd for  $\text{C}_9\text{H}_{10}\text{NO}_4^+$  196.0610, found 196.0605.

(ii) A mixture of **D** (0.20 g, 1.0 mmol) and hydrazine hydrate (0.60 mL, 10.0 mmol) was stirred in methanol (20 mL) at 65 °C for 24 h. Upon completion of the reaction, the solvent is evaporated under reduced pressure to yield the crude product, which is subsequently washed several times with methanol to obtain product **pyridine-2,5-dicarbohydrazide** as light-yellow solid in 87% yield (0.20 g). IR (KBr pellet  $\text{cm}^{-1}$ ): IR (KBr pellet  $\text{cm}^{-1}$ ): 3307 (vs), 1646 (s), 1615 (s), 1506 (s), 1417 (s), 1339 (w), 1303 (w), 1113 (w), 940 (s), 895 (w), 681 (s).  $^1\text{H}$  NMR (400 MHz,  $\text{DMSO-}d_6$ )  $\delta$  10.07 (d,  $J = 12.0$  Hz, 2H), 8.95 (m, 1H), 8.32 (dd,  $J = 8.0$  Hz, 1H), 8.05 (dd,  $J = 8.0$  Hz, 1H), 4.62 (s, 4H).  $^{13}\text{C}$  NMR (101 MHz,  $\text{DMSO-}d_6$ )  $\delta$  164.04, 162.11-159.03, 152.01, 147.48, 136.80, 131.20, 121.95. HRMS (ESI)  $m/z$   $[\text{M}+\text{H}]^+$  calcd for  $\text{C}_7\text{H}_{10}\text{N}_5\text{O}_2^+$  196.0834, found 196.0827.

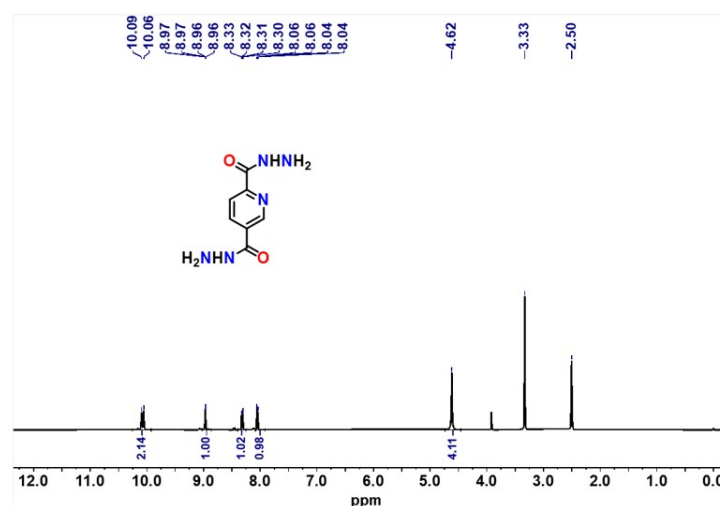
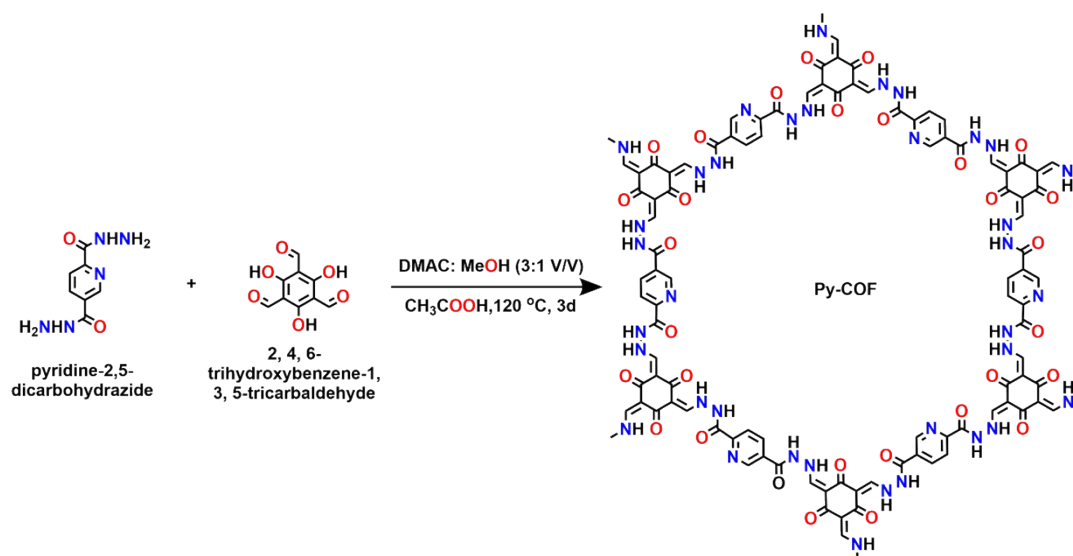


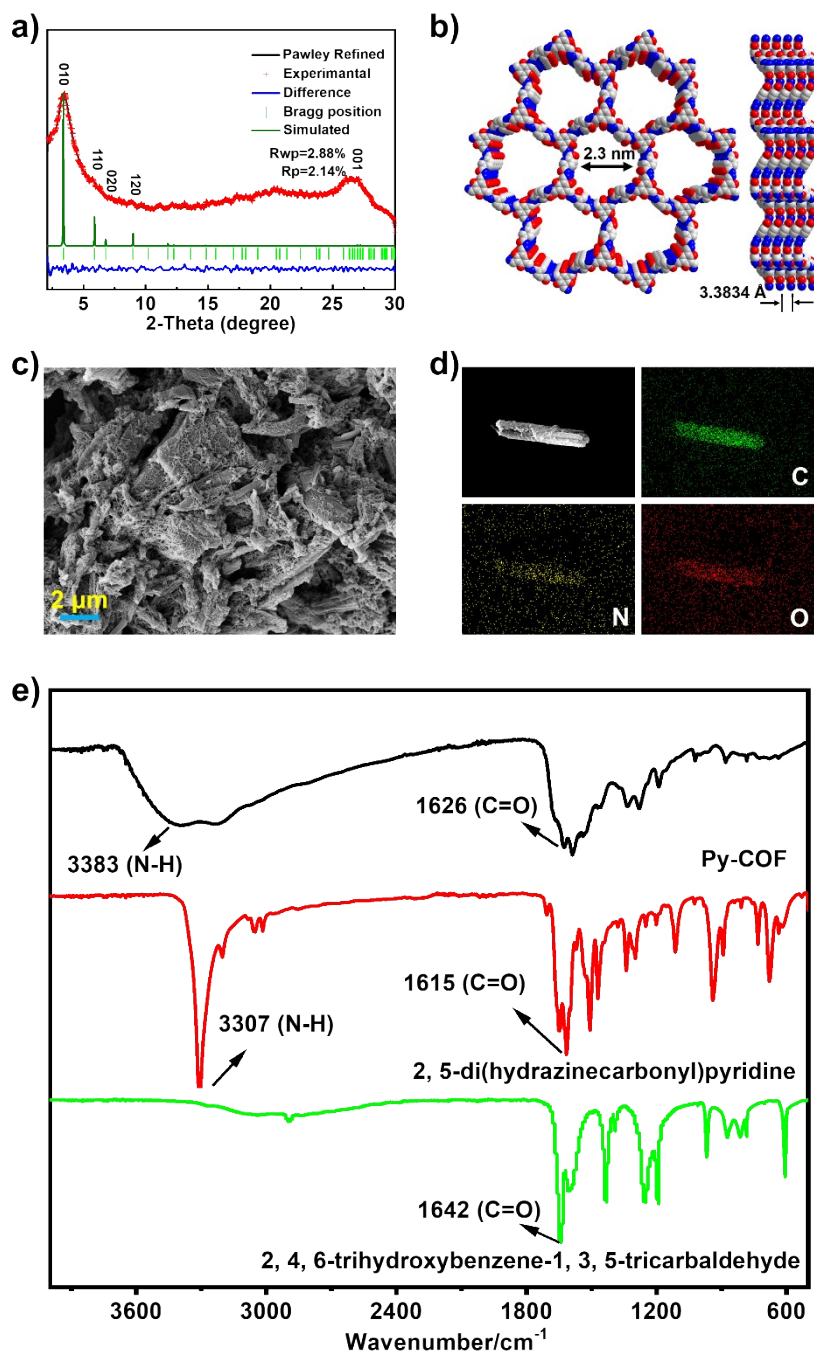
Fig. S4.  $^1\text{H}$  NMR spectra of **pyridine-2,5-dicarbohydrazide**

## (2) Synthesis and characterization of Py-COF



Scheme S3 Synthesis of **Py-COF**

A mixture of **pyridine-2,5-dicarbohydrazide** (29.3 mg, 0.15 mmol), acetic acid (0.3 mL, 6.0 M), 2,4,6-trihydroxy-1,3,5-benzenetricarbaldehyde (21.0 mg, 0.10 mmol) and N, N-dimethyl acetamide/ methanol (1.5/0.5 mL) was capped in a Pyrex tube and heated at 120 °C for 3 days. The precipitate was collected by centrifugation and washed with N, N-dimethyl formamide and ethanol, respectively. Then, the collected solid was dried in vacuo overnight to yield **Py-COF** (21.7 mg, 70% yield). IR (KBr pellet  $\text{cm}^{-1}$ ): 3384 (s), 3226 (s), 1626 (vs), 1588 (vs), 1537 (w), 1334 (s), 1280 (s), 1181 (w), 1022 (w), 875 (w).



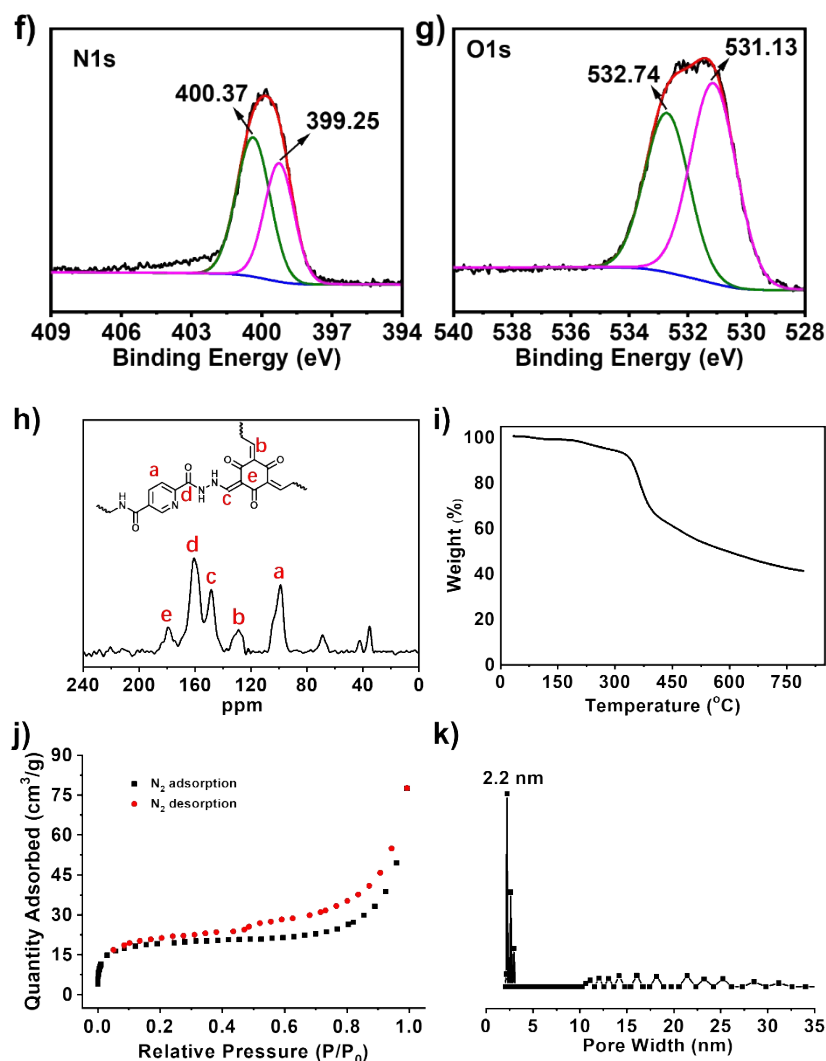


**Fig. S5.** a) PXRD patterns of **Py-COF** (AA stacking). b) The top and side views of **Py-COF** (AA stacking). c) SEM image of **Py-COF**. d) SEM-EDX images of **Py-COF**. e) The FT-IR spectra of **Py-COF** and its monomers. The FT-IR spectra showed the characteristic peaks such as  $1626\text{ cm}^{-1}$  for  $[-\text{C}=\text{O}]$ ,  $3383\text{ cm}^{-1}$  for  $[-\text{N}-\text{H}]$  stretching vibrations, which suggested the formation of **Py-COF** through Schiff base condensation. f) The XPS spectrum of N species in **Py-COF**. The XPS spectrum of N species in **Py-COF** showed that deconvolution of the N 1s spectrum resulted in two peaks at 400.37 and 399.25 eV, which can be attributed to the nitrogen atoms bound to carbon (i.e., N-C) and (i.e., N=C), respectively.<sup>3</sup> g) The XPS spectrum of O species in **Py-COF**. The XPS spectrum of O species in **Py-COF** showed that deconvolution of the O 1s spectrum also resulted in two peaks at 532.74 and 531.13 eV, which can be attributed to the oxygen atoms bound to carbon (i.e., O=C).<sup>4</sup> h) The solid-state  $^{13}\text{C}$ -MAS NMR spectrum of **Py-COF**,  $\delta$  (ppm): 182.2, 179.5, 174.3, 160.9, 153.7, 148.5, 130.1, 129.6, 98.8. The formation of **Py-COF** was verified by the existence of the keto, hydrazide, acylhydrazinyl, pyridine and alkene in **Py-COF** through the corresponding resonances at 179.5, 160.9, 148.5, 129.6, 98.8 ppm, respectively. i) TGA trace of **Py-COF**. j)  $\text{N}_2$  adsorption isotherms for **Py-COF** at 77 K.  $\text{N}_2$  adsorption at 77 K revealed absorption amounts of **Py-COF** was  $78.0\text{ cm}^3/\text{g}$ , and its surface areas calculated on basis of the BET model were determined as  $62.0\text{ m}^2/\text{g}$ . k) Pore size distribution curve of **Py-COF**. Pore size distribution curves, calculated from nonlocal density functional theory (NLDFT) analysis, showed that the pore width of **Py-COF** was centered at  $\sim 2.2\text{ nm}$ .

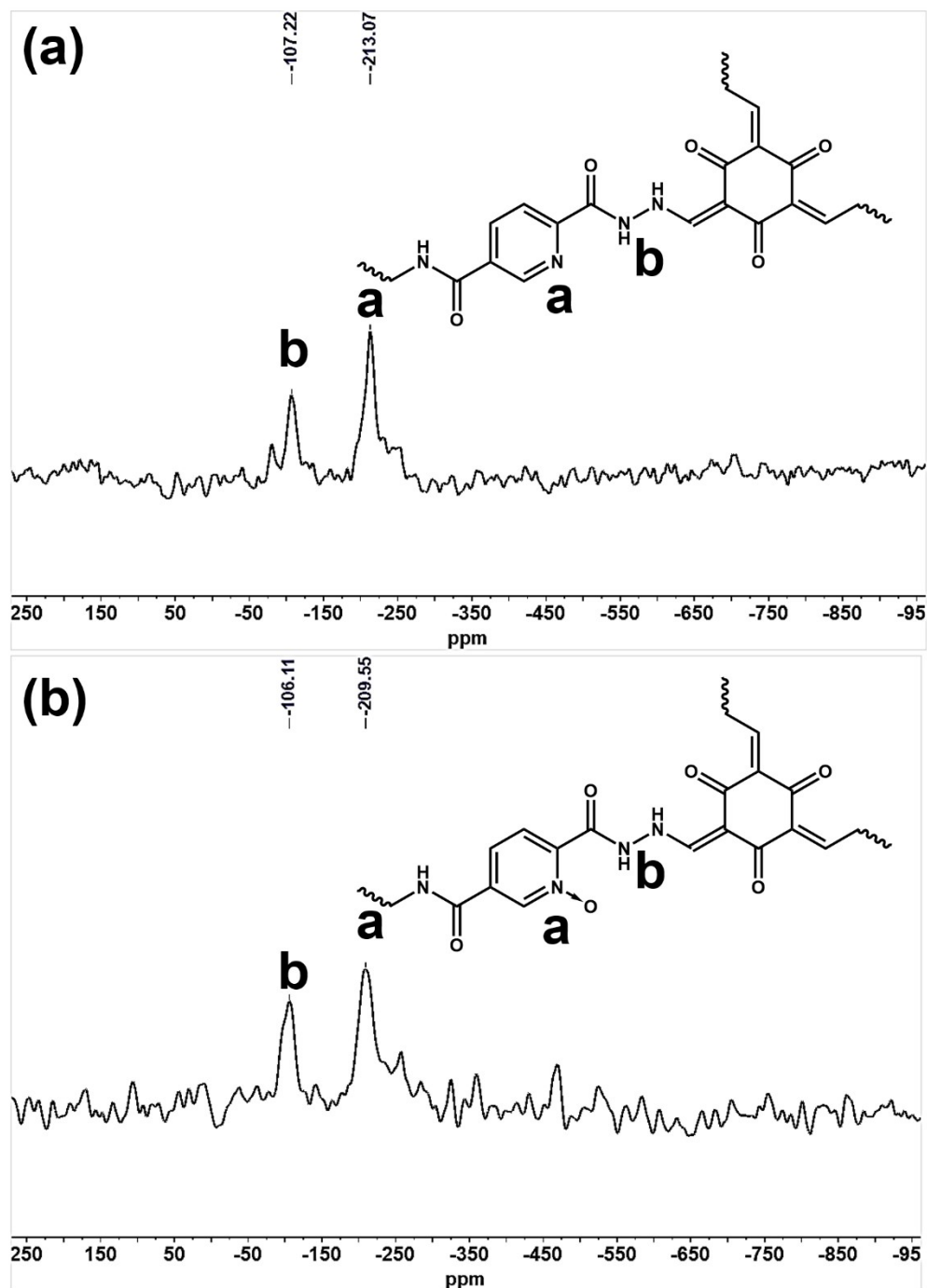
**Table S3.** Fractional atomic coordinates for the unit cell of **Py-COF****Py-COF** AA stacking mode, space group: *P3* $a = b = 30.0420 \text{ \AA}$ ,  $c = 3.3834 \text{ \AA}$  $\alpha = \beta = 90^\circ$ ,  $\gamma = 120^\circ$ 

Aotm	x	y	z
C1	-0.69738	-0.39047	0.54148
C2	-0.64053	-0.36357	0.58524
C3	-0.72652	-0.44155	0.47234
O4	-0.61921	-0.38757	0.67734
N5	-0.70595	-0.47434	0.38008
N6	-0.73845	-0.52803	0.37864
C7	-0.72019	-0.5608	0.29984
C8	-0.75545	-0.61714	0.29056
C9	-0.73658	-0.65112	0.24233
C10	-0.77078	-0.70398	0.23312
C11	-0.82383	-0.72318	0.27352
C12	-0.84112	-0.68784	0.31679
N13	-0.80705	-0.63655	0.32552
O14	-0.67443	-0.5435	0.23779
C16	-0.86135	-0.77908	0.25956
N17	-0.84844	-0.81448	0.39116
N18	-0.88173	-0.86805	0.37338
C19	-0.93498	-0.89229	0.48794
C20	-0.96488	-0.94334	0.55583
O21	-0.90403	-0.79327	0.12513
C22	-0.94414	-0.97882	0.60077
O23	0.10059	0.03786	0.6967
H24	0.33154	0.54119	0.27488
H25	0.22264	0.45692	0.4448
H26	0.30418	0.36299	0.20947
H27	0.24443	0.27058	0.18449
H28	0.1183	0.29901	0.34721
H29	0.86869	0.91601	0.50518



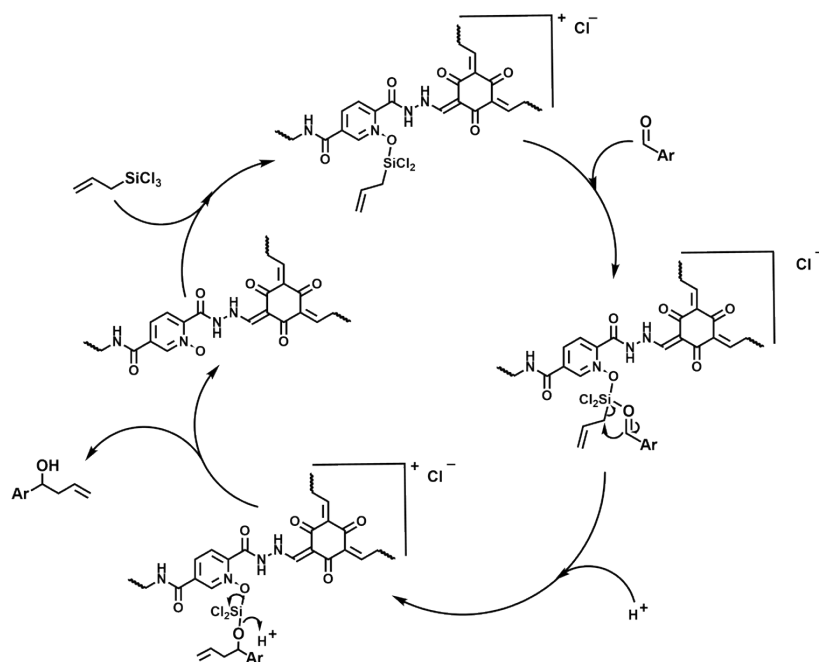
H30	0.80186	0.99069	0.49162
H31	0.9752	0.8653	0.2921
H32	0.45894	0.69095	0.46855

## 6. The solid-state $^{15}\text{N}$ NMR spectra of Py-O-COF and Py-O-COF



**Fig. S6.** (a) The solid-state  $^{15}\text{N}$  NMR spectrum of Py-COF,  $\delta$  (ppm): -107.22 (-NH-), -213.07 (-C=N-). (b) The solid-state  $^{15}\text{N}$  NMR spectrum of Py-O-COF,  $\delta$  (ppm): -106.11 (-NH-), -209.55 (-C=N-O). The formation of Py-O-COF was verified by the significant chemical shift disparities of the nitrogen in pyridine in Py-COF and oxidized pyridine in Py-O-COF.

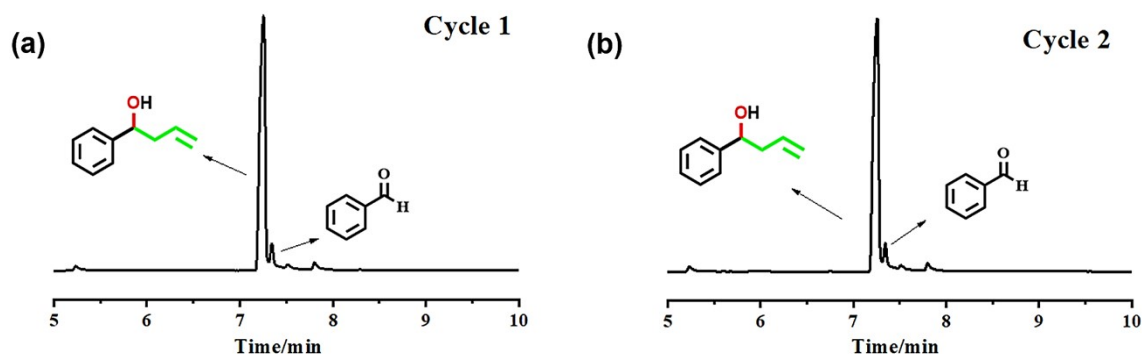
## 7. A possible reaction mechanism of Py-O-COF-catalyzed the allylation of benzaldehyde



**Fig. S7.** A possible reaction mechanism of Py-O-COF-catalyzed the allylation of benzaldehyde. The results of previous reports suggest that the allylations of aromatic and unsaturated aldehydes mediated by the pyridine oxide units in Py-O-COF via cyclic chairlike transition structures, involving hypervalent silicates where one of a pair of N-oxide moieties occupies an axial position.

## 8. GC analysis for five catalytic runs of the allylation of benzaldehyde and N<sub>2</sub> adsorption isotherms for Py-O-COF at 77 K before and after five catalytic runs

In nitrogen, a mixture of benzaldehyde (0.30 mmol), allyltrimethylsilane (0.36 mmol), DIPEA (0.90 mmol), Py-O-COF (20 mg), and CH<sub>3</sub>CN (2.0 mL) was stirred at 25 °C for 48 h. GC was used to monitor the reaction progress. After reaction, the solid catalyst was recovered by centrifugation, washed with ethanol and dried overnight for the next cycle. The mixture was quenched with saturated brine and extracted with ethyl acetate. Then, the combined organic layers were evaporated in vacuo and the resulting residue was purified by silica gel chromatography (petroleum ether/ethyl acetate = 3/1).



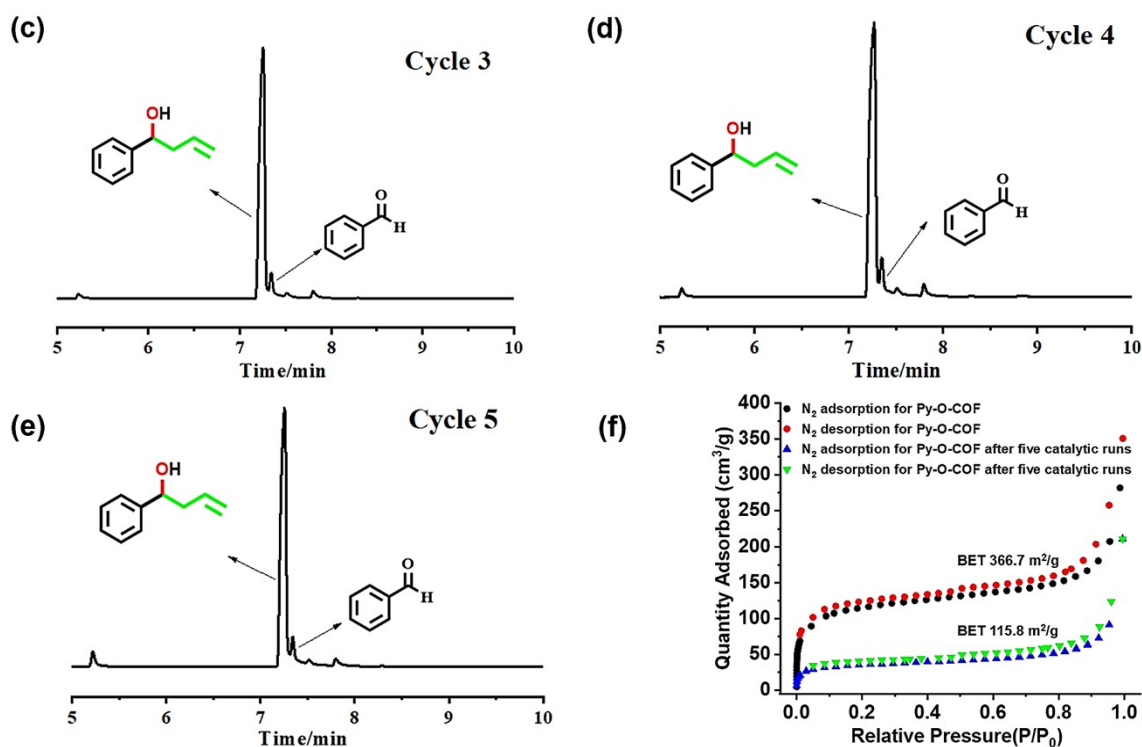


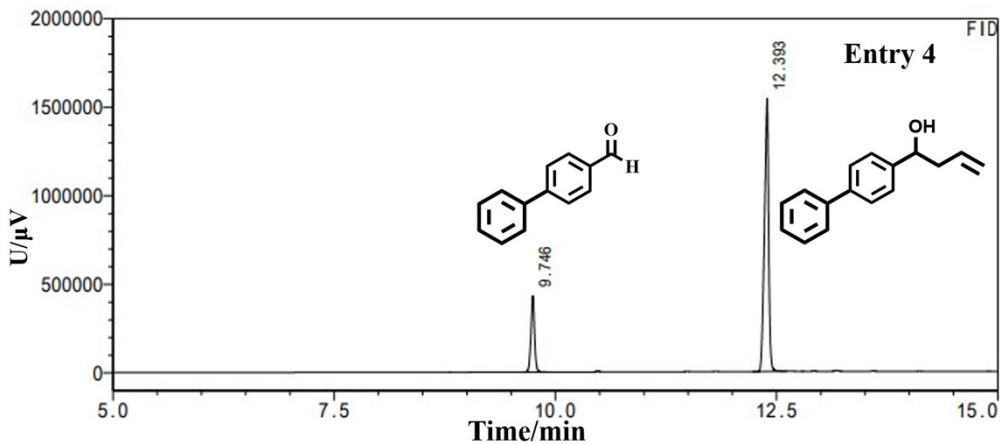
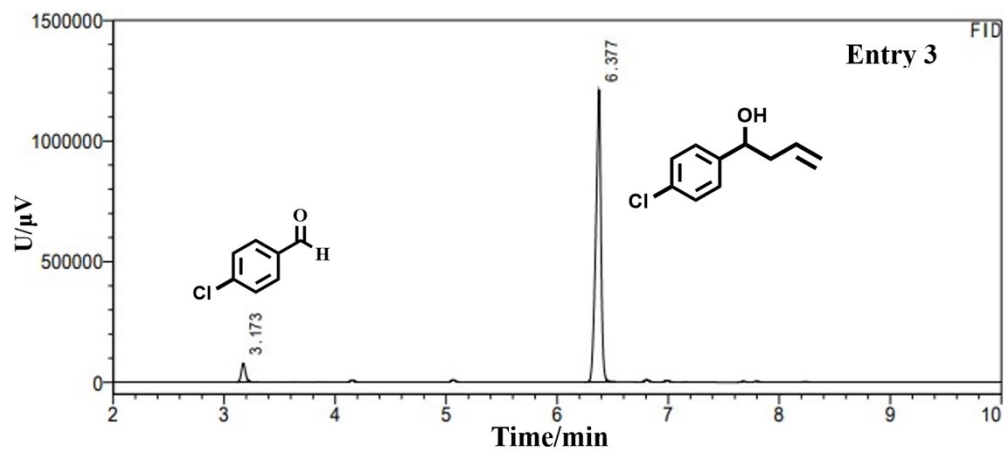
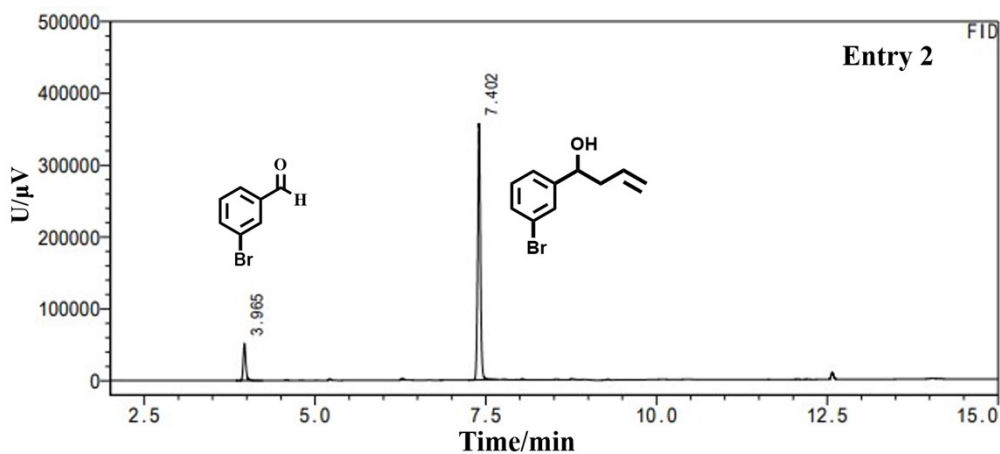
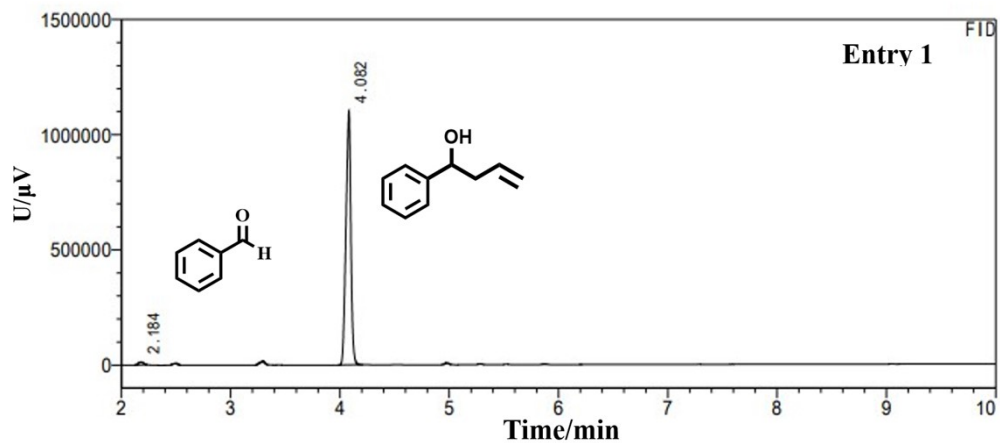
**Fig. S8.** Yields of the model reaction for five catalytic runs was determined by GC. (a-e) GC analysis for five catalytic runs of the allylation of benzaldehyde. (f)  $N_2$  adsorption isotherms for **Py-O-COF** at 77 K before and after five catalytic runs.

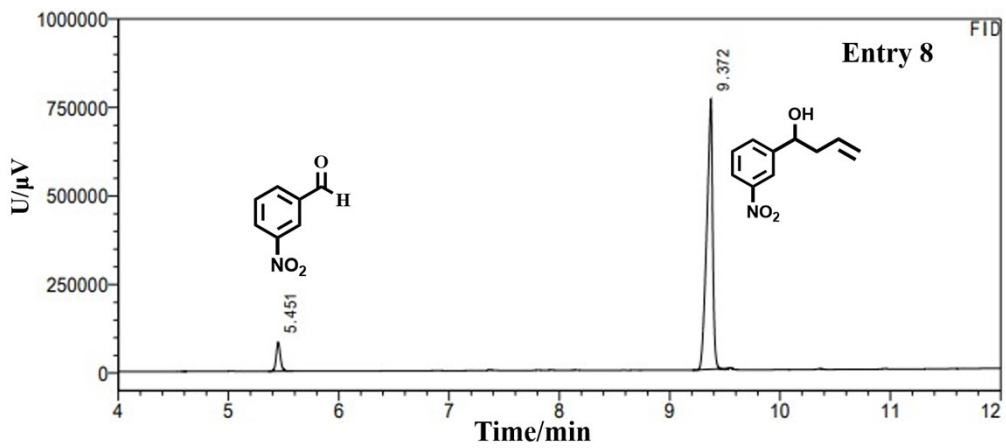
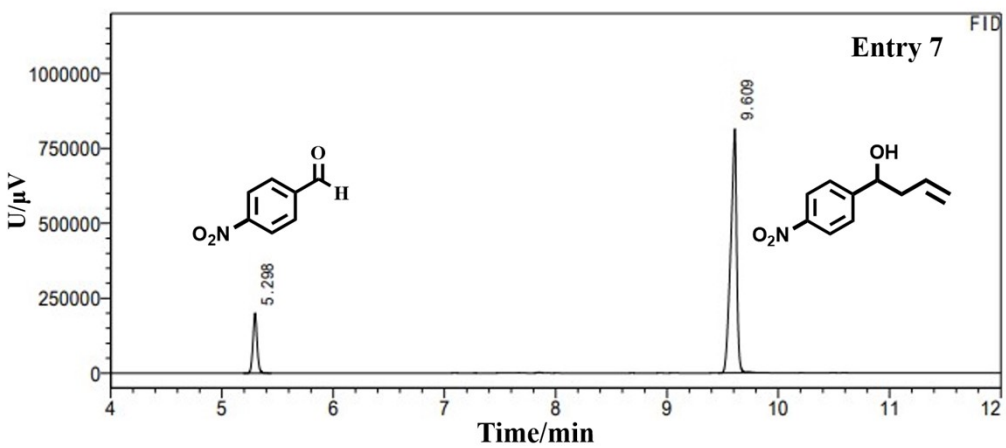
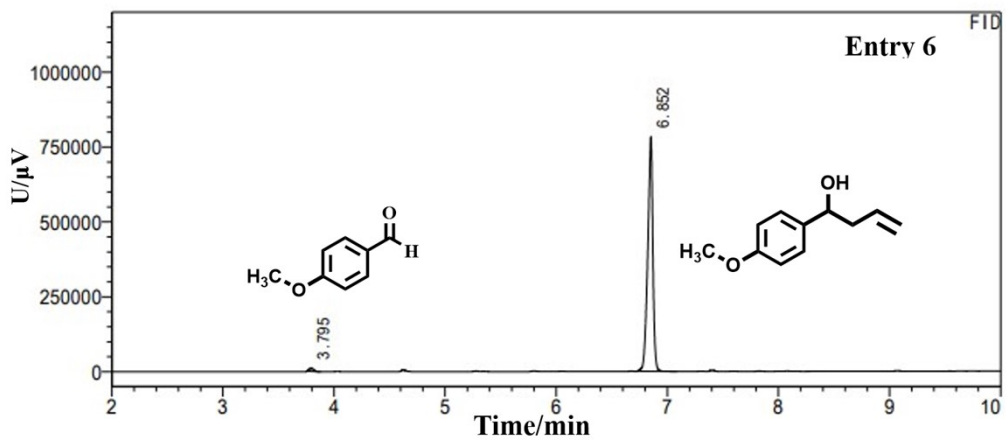
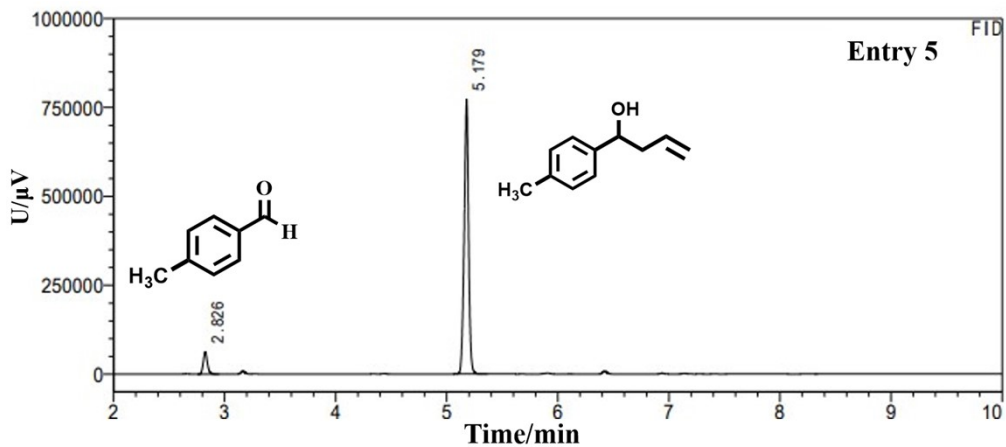
## 9. Comparison of **Py-O-COF** with some reported catalysts for allylation of aromatic aldehyde

**Table S4.** Comparison of **Py-O-COF** with some reported catalysts for allylation of aromatic aldehyde.

Entry	Catalyst	T/°C	Time/h	Solvent	Yield/%	Reusability	Ref.
1	PIB-pyridyl N-oxide	40	48	$CH_2Cl_2$	74	5	5
2	methyl p-tolyl sulfoxide	-78	8	$CH_2Cl_2$	49	/	6
3	PIB-HMPA	25	26	$CH_3CN$	97	5	7
4	chiral sulfoxides	-78	48	$CH_2Cl_2$	67	/	8
5	phosphine oxide aziridinyl phosphonate	25	24	$CH_3CN$	78	/	9
6	TetraPh-Tol-BITIOPO	0	48	$CH_3CN$	87	/	10
7	<b>Py-O-COF</b>	25	48	$CH_3CN$	99	5	<b>This work</b>

## 10. GC analysis for the reactions **Py-O-COF**-catalyzed different substituted aromatic aldehydes and allyl trichlorosilane as substrates (Table 2)





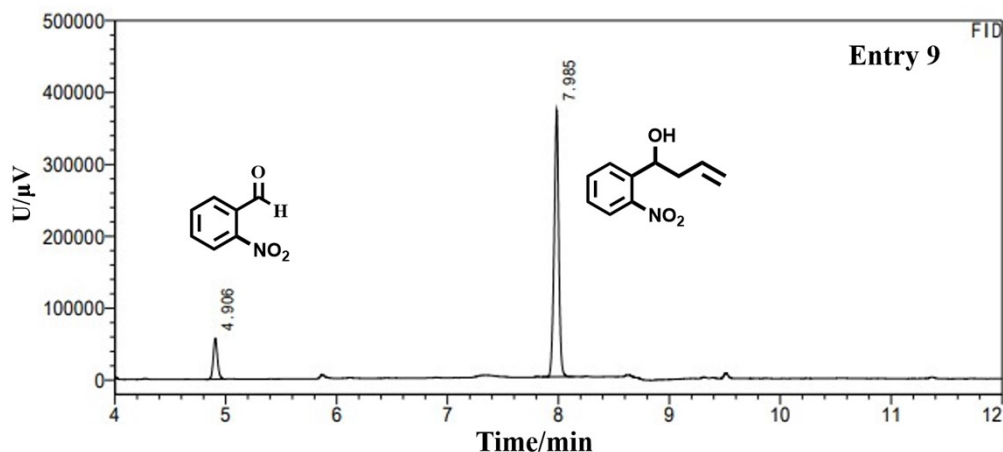
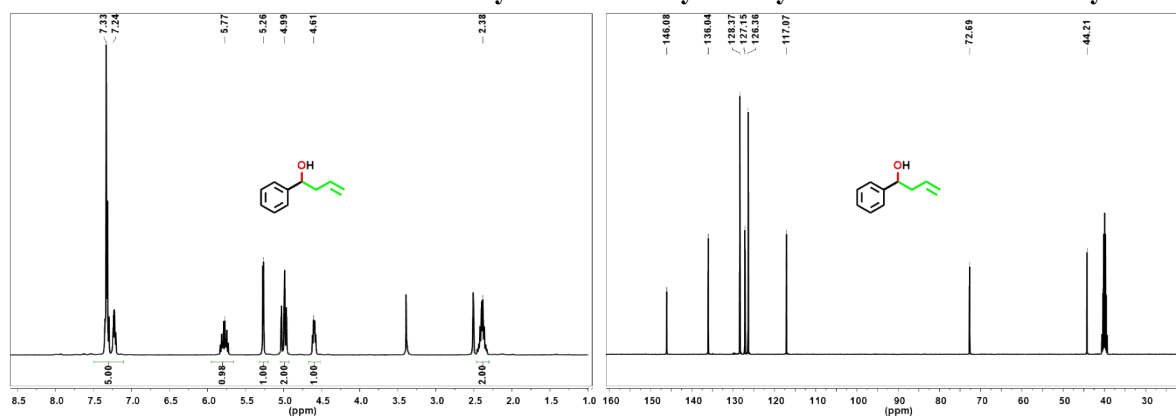
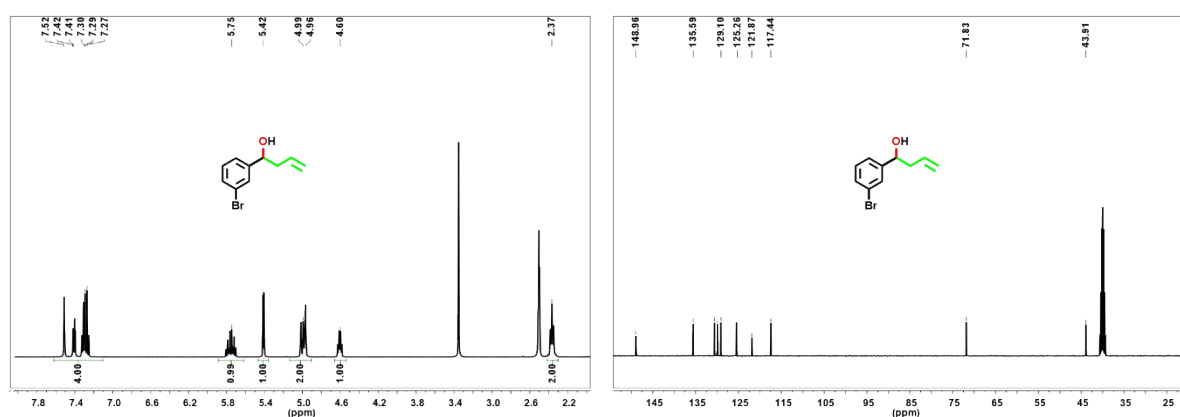


**Fig. S9.** Yields of the reactions Py-O-COF-catalyzed different substituted aromatic aldehydes and allyl trichlorosilane as substrates were determined by GC.

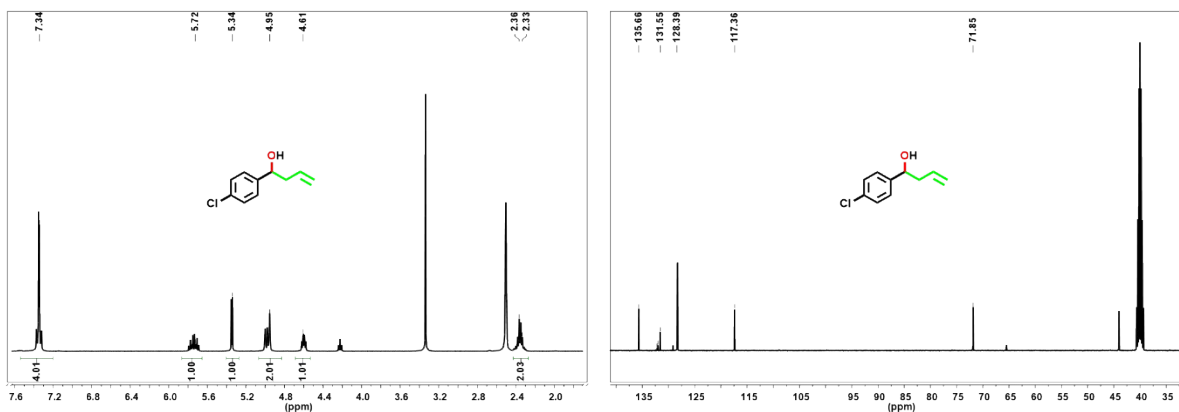
### 11. Products characterization for the Py-O-COF catalyzed allylation of aromatic aldehyde



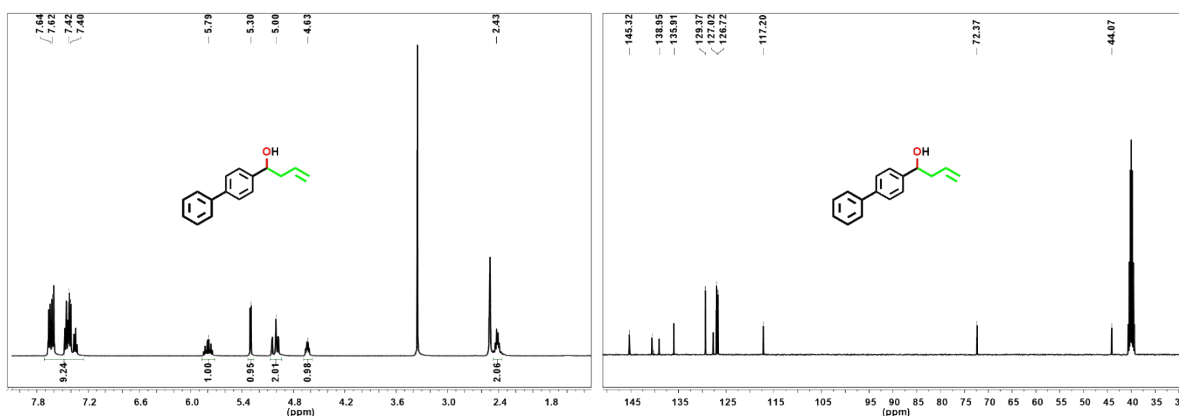
$^1\text{H}$  NMR (400 MHz,  $\text{DMSO-}d_6$ )  $\delta$  7.28 (d,  $J = 36.1$  Hz, 5H), 5.77 (s, 1H), 5.26 (s, 1H), 4.99 (s, 2H), 4.61 (s, 1H), 2.38 (s, 2H).  $^{13}\text{C}$  NMR (101 MHz,  $\text{DMSO-}d_6$ )  $\delta$  146.08, 136.04, 128.37, 127.15, 126.36, 117.07, 72.69, 44.21. HRMS (ESI)  $m/z$   $[\text{M-H}]^-$  calcd for  $\text{C}_{10}\text{H}_{11}\text{O}^-$  147.0815, found 147.0432.



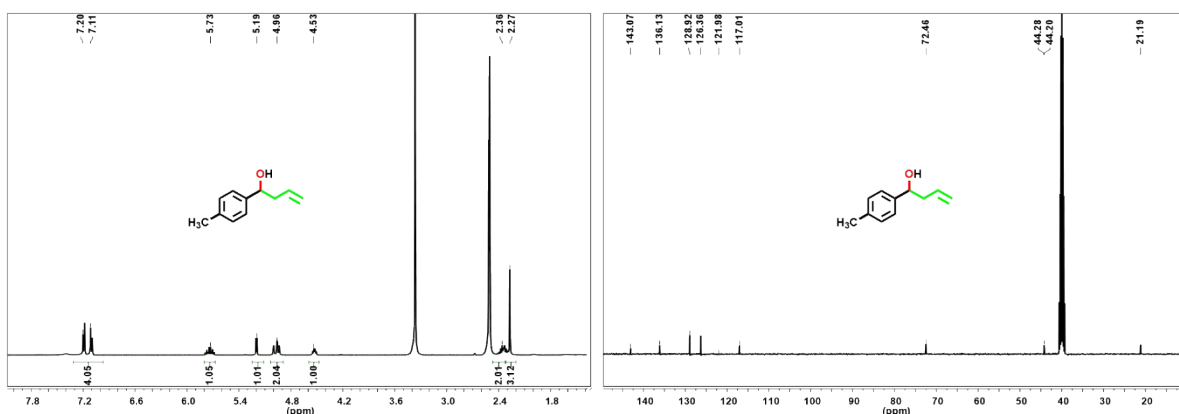
$^1\text{H}$  NMR (400 MHz,  $\text{DMSO-}d_6$ )  $\delta$  7.62-7.11 (m, 4H), 5.75 (s, 1H), 5.42 (s, 1H), 4.98 (d,  $J = 12.6$  Hz, 2H), 4.60 (s, 1H), 2.37 (s, 2H).  $^{13}\text{C}$  NMR (101 MHz,  $\text{DMSO-}d_6$ )  $\delta$  148.96, 135.59, 130.62, 129.95, 129.10, 125.48, 121.87, 117.44, 71.83, 43.91. HRMS (ESI)  $m/z$   $[\text{M-H}]^-$  calcd for  $\text{C}_{10}\text{H}_{10}\text{BrO}^-$  224.9915, found 225.0014.



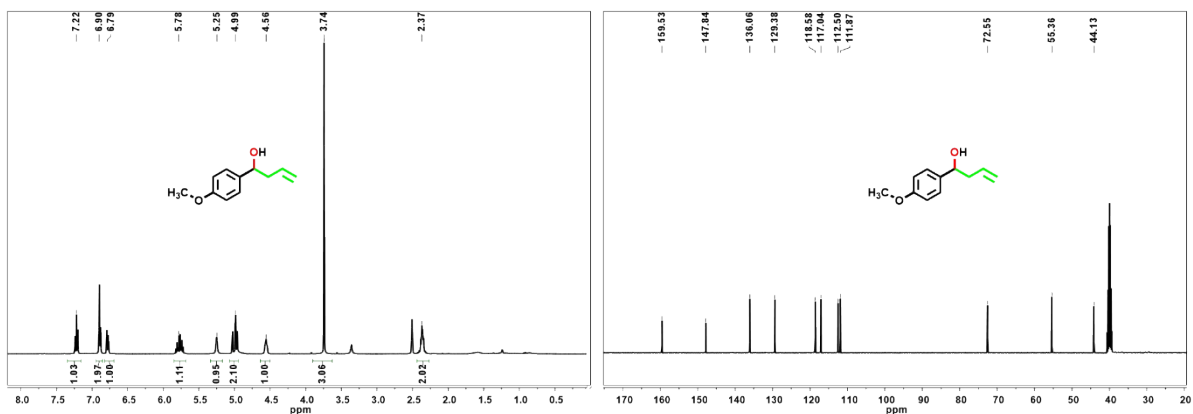
$^1\text{H}$  NMR (400 MHz,  $\text{DMSO-}d_6$ )  $\delta$  7.34 (s, 4H), 5.72 (s, 1H), 5.34 (s, 1H), 4.95 (s, 2H), 4.61 (s, 1H), 2.35 (d,  $J = 12.7$  Hz, 2H).  $^{13}\text{C}$  NMR (101 MHz,  $\text{DMSO-}d_6$ )  $\delta$  145.03, 135.66, 132.62, 128.39, 117.52, 71.85, 43.90. HRMS (ESI)  $m/z$   $[\text{M-H}]^-$  calcd for  $\text{C}_{10}\text{H}_{10}\text{ClO}^-$  181.0420, found 181.0515.



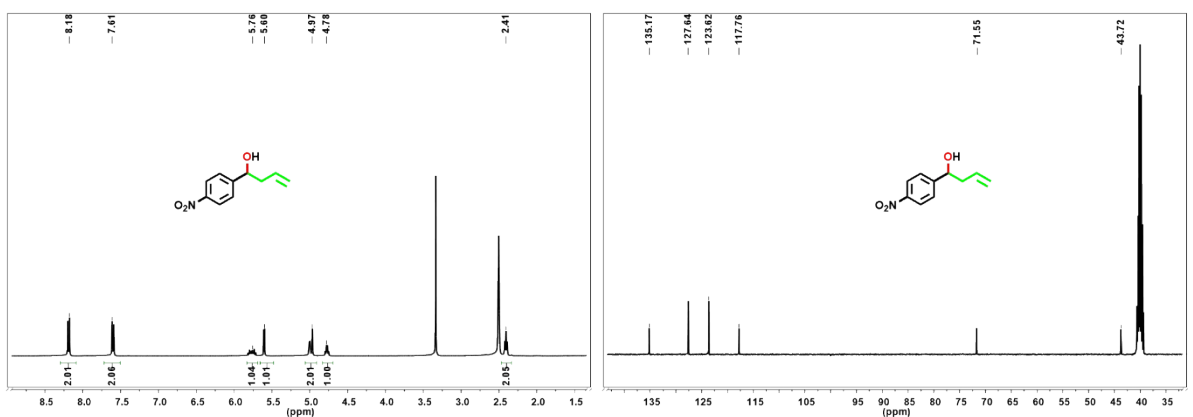
$^1\text{H}$  NMR (400 MHz,  $\text{DMSO-}d_6$ )  $\delta$  7.52 (dd,  $J = 7.2$  Hz, 9H), 5.79 (s, 1H), 5.30 (s, 1H), 5.00 (s, 2H), 4.63 (s, 1H), 2.43 (s, 2H).  $^{13}\text{C}$  NMR (101 MHz,  $\text{DMSO-}d_6$ )  $\delta$  145.32, 140.56, 138.95, 135.91, 129.37, 127.02, 126.72, 117.20, 72.37, 44.07. HRMS (ESI)  $m/z$   $[\text{M-H}]^-$  calcd for  $\text{C}_{16}\text{H}_{15}\text{O}^-$  223.1123, found 223.1107.



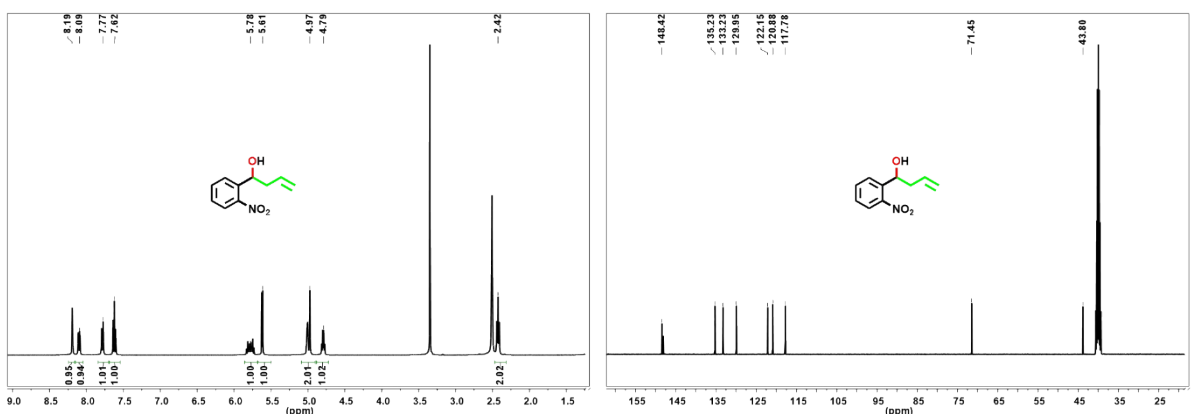
$^1\text{H}$  NMR (400 MHz,  $\text{DMSO-}d_6$ )  $\delta$  7.16 (d,  $J = 34.9$  Hz, 4H), 5.73 (s, 1H), 5.19 (s, 1H), 4.96 (s, 2H), 4.53 (s, 1H), 2.36 (s, 2H), 2.27 (s, 3H).  $^{13}\text{C}$  NMR (101 MHz,  $\text{DMSO-}d_6$ )  $\delta$  143.07, 136.13, 128.92, 126.36, 117.01, 72.46, 44.20, 21.04. HRMS (ESI)  $m/z$   $[\text{M}+\text{Na}]^+$  calcd for  $\text{C}_{11}\text{H}_{14}\text{ONa}^+$  185.0942, found 185.0999.



$^1\text{H}$  NMR (400 MHz,  $\text{DMSO-}d_6$ )  $\delta$  7.22 (s, 1H), 6.90 (s, 2H), 6.79 (s, 1H), 5.78 (s, 1H), 5.25 (s, 1H), 4.99 (s, 2H), 4.56 (s, 1H), 3.74 (s, 3H), 2.37 (s, 2H).  $^{13}\text{C}$  NMR (101 MHz,  $\text{DMSO-}d_6$ )  $\delta$  159.53, 147.84, 136.06, 129.38, 118.58, 117.04, 112.50, 111.87, 72.55, 55.36, 44.13. HRMS (ESI)  $m/z$   $[\text{M}+\text{Na}]^+$  calcd for  $\text{C}_{11}\text{H}_{14}\text{O}_2\text{Na}^+$  201.0891, found 201.0869.

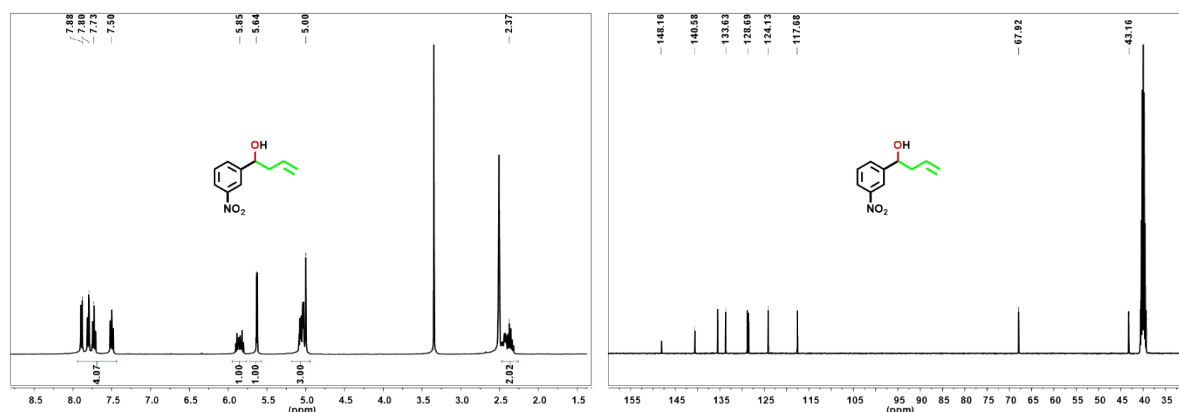


$^1\text{H}$  NMR (400 MHz,  $\text{DMSO-}d_6$ )  $\delta$  8.18 (s, 2H), 7.61 (s, 2H), 5.76 (s, 1H), 5.60 (s, 1H), 4.97 (s, 2H), 4.78 (s, 1H), 2.41 (s, 2H).  $^{13}\text{C}$  NMR (101 MHz,  $\text{DMSO-}d_6$ )  $\delta$  135.17, 127.64, 123.62, 117.76, 43.72. HRMS (ESI)  $m/z$   $[\text{M}-\text{H}]^-$  calcd for  $\text{C}_{10}\text{H}_{10}\text{NO}_3^-$  192.0661, found 192.0611.



$^1\text{H}$  NMR (400 MHz,  $\text{DMSO-}d_6$ )  $\delta$  8.19 (s, 1H), 8.09 (s, 1H), 7.77 (s, 1H), 7.62 (s, 1H), 5.78 (s, 1H), 5.61 (s, 1H), 4.97 (s, 2H), 4.79 (s, 1H), 2.42 (s, 2H).  $^{13}\text{C}$  NMR (101 MHz,  $\text{DMSO-}d_6$ )  $\delta$  148.42, 135.23, 133.23, 129.95, 122.15, 120.88, 117.78, 71.45, 43.80. HRMS (ESI)  $m/z$   $[\text{M}-\text{H}]^-$  calcd for  $\text{C}_{10}\text{H}_{10}\text{NO}_3^-$  192.0661, found 192.0660.





$^1\text{H}$  NMR (400 MHz,  $\text{DMSO-}d_6$ )  $\delta$  7.73 (dd,  $J = 61.8$  Hz, 4H), 5.85 (s, 1H), 5.64 (s, 1H), 5.00 (s, 3H), 2.37 (s, 2H).  $^{13}\text{C}$  NMR (101 MHz,  $\text{DMSO-}d_6$ )  $\delta$  148.16, 140.58, 135.59, 133.63, 128.69, 124.13, 117.68, 67.92, 43.16. HRMS (ESI)  $m/z$   $[\text{M-H}]^-$  calcd for  $\text{C}_{10}\text{H}_{10}\text{NO}_3^-$  192.0661, found 192.0657.

**Fig. S10.**  $^1\text{H}$  NMR spectra and  $^{13}\text{C}$  NMR spectra of all products obtained by the **Py-O-COF**-catalyzed allylation of aromatic aldehyde.

## 12. Reference

1. J. C. Wang, C. X. Liu, X. Kan, X. W. Wu, J. L. Kan and Y. B. Dong, *Green. Chem.*, 2020, **22**, 1150-1155.
2. J. Y. Cheng, F. W. Ding, P. Wang, C. W. Zhao and Y. B. Dong, *ChemPlusChem*, 2016, **81**, 743-751.
3. (a) X.-L. Chen, M. Xie, Z.-L. Zheng, X. Luo, H. Jin, Y.-F. Chen, G.-Z. Yang, D.-S. Bin, D. Li. *J. Am. Chem. Soc.* 2023, **145**, 5105-5113. (b) Y. Yang, H. Huang, C. Yang, H. He. *ACS Appl. Energ. Mater.* 2021, **4**, 376-383. (c) B. Liu, S. Xue, S. Tan, D. Zhang, Z. Deng, H. Pan, W. Tu, R. Zhang, H. Zhang, Y. Wang. *Energ. Fuel.* 2022, **36**, 4532-4540. (d) C. Karaman. *Top. Catal.*, 2021, **65**, 656-667.
4. S. Kundu, Y. Wang, W. Xia, M. Muhler. *J. Phys. Chem. C.*, 2008, **112**, 16869-16878.
5. D. E. Bergbreiter, D. Ortiz-Acosta. *Tetrahedron Lett.*, 2008, **49**, 5608-5610.
6. V. DeSio, A. Massa, A. Scettri. *Org Biomol Chem.*, 2010, **8**, 3055-3059.
7. Y. H. Fu, D. E. Bergbreiter. *ChemCatChem.*, 2020, **12**, 6050-6058.
8. G. J. Rowlands, W. Kentish Barnes. *Chem. Commun.*, 2003, **21**, 2712-2713.
9. Ö. Dogan, A. Bulut, M. A. Tecimer. *Tetrahedron: Asymmetry*, 2015, **26**, 966-969.
10. A. V. Mirco, B. Maurizio, R. Sergio, B. Tiziana, C. Roberto, P. Marco. *Org. Biomol. Chem.*, 2019, **17**, 7474-7481.